The Thesis Committee for Athreya Suresh Babu
Certifies that this is the approved version of the following Thesis:

NITROGEN DIOXIDE ABSORPTION INTO AQUEOUS SULFITE INHIBITED BY THIOSULFATE

APPROVED BY
SUPERVISING COMMITTEE:

Desmond F. Lawler, Supervisor

Gary T. Rochelle

NITROGEN DIOXIDE ABSORPTION INTO SULFITE INHIBITED BY THIOSULFATE

by

Athreya Suresh Babu

Thesis

Presented to the Faculty of the Graduate School of

The University of Texas at Austin

in Partial Fulfillment

of the Requirements

for the Degree of

Master of Science in Engineering

The University of Texas at Austin

August, 2019

Dedication

To my family

Acknowledgements

First and foremost, I am most grateful to Professor Gary T. Rochelle for his unending support and guidance throughout this project work. I have enjoyed every weekly meeting with him and his contagious love for the subject has inspired me. By doing research under him, I have become a more environmentally aware chemical engineer. I am excited to continue this journey as a Ph.D. student in his group.

I am also thankful to Professor Desmond F. Lawler for always making time for discussions despite his busy schedule and travel. Turbidity measurements made in this research would not have been possible without the support of Dr. Lawler and his graduate student, Matt Landsman. I also enjoyed taking his course on physical and chemical water treatment processes. It was very demanding, but I learnt a great deal.

This work was supported by the Texas Carbon Management Program, and by the Department of Energy under Award Number DE-FE0005654, and by the Carbon Capture Project (CCP4). I thank our colleagues at The National Carbon Capture Center who provided expertise that greatly benefited the pilot plant campaigns, with special thanks to Karen Farmer, Graham Bingham, and Laura Uhrig for their time and effort.

Members of the Rochelle Group have been a pleasure to work with. I would like to thank Dr. Kent Fischer and Yuying Wu for helping me set up equipment and gas lines around the lab, teaching me sample preparation, procuring pilot plant samples, and always making sure that the IC was troubleshot. Joe Selinger did most of the work that this research was based on and I am thankful for that. I thank Ching-Ting Liu, Tianyu Gao, and Korede Akinpelumi for being great friends; I enjoyed your company when we were TAs for the senior design course.

Special thanks go to Maeve Cooney for always patiently editing my quarterly reports and for being the backbone of the Rochelle Group. I think I am becoming a better writer with your help.

My father, mother, and brother have sacrificed a lot for my education, and I will always be thankful for that. I am also grateful for the company of the great friends I have made in Austin. Thank you for being my family away from home.

Finally, I would like to thank The Almighty God for giving me the strength and ability to undertake this research study and to persevere and complete it satisfactorily.

Abstract

NITROGEN DIOXIDE ABSORPTION INTO SULFITE INHIBITED BY THIOSULFATE

Athreya Suresh, M.S.E.

The University of Texas at Austin, 2019

Supervisor: Desmond F. Lawler

Emulsified sulfur was found to be the most suitable form of sulfur for in-situ thiosulfate production for sulfite inhibition with a maximum sulfur-to-thiosulfate-conversion of 50 % and t_{50} of 6 hours. Increasing the ionic strength of the solution reduces the reaction rate between sulfur and sulfite. Reaction rate reduced by 3 when ionic strength of the solution was increased from 0.225 M to 2.95 M. The rate of reaction between sulfur and sulfite was found to be first-order in sulfur, half-order in sulfite, and zero-order in thiosulfate with a reaction rate constant of 5.48×10^{-3} $mM^{-0.5}$ min^{-1}. Increasing the reaction temperature from 40 to 75 °C increased the interpreted reaction rate by a factor of 17. The activation energy of the reaction was found to be 74.2 kJ/mol, and this high value indicates that the reaction might be kinetically limited and not mass transfer limited. The reaction rate model predicts experimental bench-scale reaction rates with an absolute average deviation of 6.5%.

In the pilot-scale prescrubber, at coal conditions, pH was observed to decrease as a function of time with 3 linear regions. These regions corresponded to CO_2 absorption to

form carbonate, conversion of carbonate to bicarbonate, and CO_2 liberation from solution by reaction of bicarbonate with SO_2 respectively. The characteristic times of these linear regions corresponded to the rate of the reaction in each of these regions. Rate of oxidation of thiosulfate under 0-1 ppm NO_2 conditions was 0.13 gmol/hr which was half the rate at 0-5 ppm NO_2 conditions. Thiosulfate loss by tank bleed was found to be directly related to the amount of gas processed. Thiosulfate loss by bleed reduced from 60 gmol to 17.2 gmol when the flue gas flow rate reduced by 1/2.25 due to the lesser amount of water condensing in the prescrubber. A minimum of 25 mM sulfite was required to maintain NO_2 removal of 90% even under low NO_2 conditions.

At NGCC conditions, thiosulfate degradation rates were 0.112 gmol/hr and 0.127 gmol/hr before and after thiosulfate addition respectively. Sulfite and thiosulfate in the prescrubber increased with SO_2 coming into the prescrubber. Thiosulfate and sulfite were correlated by a power-law relation just as in the coal condition.

Table of Contents

List of Tables

List of Figures

Chapter 1: Introduction

Post-combustion CO_2 capture by amine scrubbing is the technology of choice to reduce emissions for coal and natural gas fired power plants. However, commercial implementation of amine scrubbing is challenged by the oxidation of amine by NO_2 in the flue gas. NO_2 will also react with secondary amines to produce nitrosamine, typically a carcinogen. Piperazine, a second-generation secondary amine, forms mononitrosopiperazine and dinotrosopiperazine on reacting with nitrosating agents such as NO_2.

Control methods that may be considered for nitrosamine management are high temperature decomposition, thermal reclaiming, hydrogenation, and UV photolysis. These methods can be limited by the relatively low operating temperature of amines or by the requirement for additional equipment. An alternative approach is to remove NO_2 or NO_x before the absorber. Selective Catalytic Reduction (SCR) is used in modern coal-fired power plants to reduce total NO_x to levels of 10 to 50 ppm. In this work NO_2 is removed simultaneously with SO_2 by sodium hydroxide scrubbing.

In the SO_2 polishing scrubber, SO_2 is absorbed from the flue gas into the liquid phase as sulfite. The sulfite in turn reacts with the incoming NO_2 to form nitrite in solution through a free-radical mechanism. As a consequence of this free radical mechanism, per mole of NO_2, multiple moles of sulfite are oxidized to sulfate (Littlejohn et al., 1993). The oxidation of sulfite decreases the amount of sulfite in the liquid phase available for NO_2 removal. Thiosulfate, a free-radical scavenger, has been identified as an effective oxidation inhibitor by providing an alternate mechanism for the termination of the free radical mechanism (Owens, 1984). Thiosulfate has been tested at both the bench-scale (Fine, 2015) and the pilot-scale (Selinger, 2018) and has been found to effectively inhibit the oxidation

of sulfite. At the pilot-scale, 50 mM thiosulfate was required to maintain the sulfite at 25 mM to remove 90 % of the incoming NO_2 (Selinger, 2018).

An economic evaluation of the polishing scrubber was done by Fine (2015). He concluded that NO_2 scrubbing using sulfite inhibited by thiosulfate was only economical with high inlet SO_2 due to the increased formation of liquid phase sulfite. Moreover, the savings realized from NO_2 prescrubbing were found to be defined by the balance between unrealized PZ losses and the cost of thiosulfate required for oxidation inhibition. The savings can be increased by producing thiosulfate on-site using emulsified sulfur (Lee and Benson, 1990).

The specific objectives of this research work are as follows:

1. To utilize emulsified sulfur to produce thiosulfate *in situ* for applications in SO_2 polishing scrubber.
2. Test the effect of ionic strength, pH, and temperature on the rate of reaction between sulfur and sulfite at the bench-scale.
3. Design and conduct factorial experiments to develop a reaction rate law for the reaction of sulfur with sulfite.
4. Modify the bench-scale test apparatus to conduct long-term simulations of the pilot-scale prescrubber at the National Carbon Capture Center.
5. Use thiosulfate as an oxidation inhibitor at the National Carbon Capture Center under both coal and natural gas conditions to test the effect of buffer tank hold-up and pH on NO_2 removal and sulfite oxidation.

The upcoming sections consist of a background chapter, methods chapter, results chapter followed by conclusions, and recommendations. In the background chapter, important literature pertinent to this research has been reviewed. A brief timeline of the research done in this area by the Rochelle Research Group has also been given. In the

methods chapter, the experimental and analytical methods that were used in this research have been explained in detail. The results chapter discuss the results of the various experiments that were done in this research. Finally, important conclusions drawn from these results and suggestions for future work are given in the final chapter.

Chapter 2: Background

2.1 The need to capture acid gases

CO_2 emissions from coal-fired power plants are the largest source of greenhouse gas (GHG) emissions in the United States. It accounts for about a fifth of the total GHG emissions (Energy Information Agency, 2012). Several technologies are being investigated to economically capture and sequester CO_2. Post-combustion CO_2 capture by amine scrubbing is the only technology that has been successfully demonstrated at a commercial scale. This dominance is due to its high thermodynamic efficiency and technological maturity. In amine scrubbing, a CO_2 lean solvent absorbs CO_2 from flue gas in an absorber to produce a CO_2 rich solvent, which liberates CO_2 at elevated temperature in the stripper (Figure 2.1). The lean solvent is recycled back to the absorber. The CO_2 is compressed and stored underground in saline aquifers.

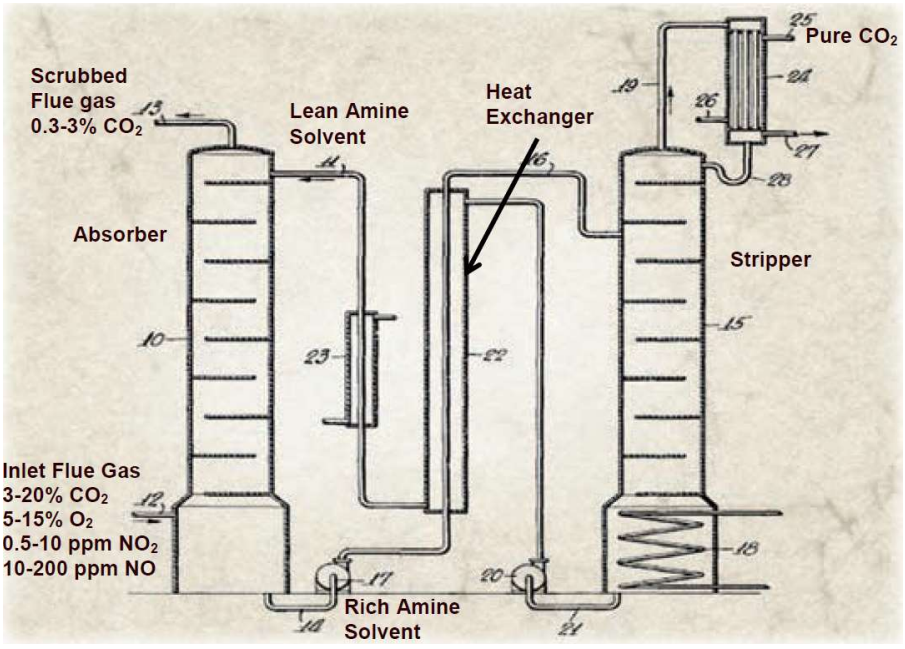

Figure 2.1: Simplified amine scrubbing process (Bottoms, 1930)

An obstacle to the commercialization of amine scrubbing is the formation of nitrosamine, a family of carcinogens that are formed by the degradation of the amine at high temperature. More than 80% of nitrosamines are harmful to human beings even at low concentration due to their reactivity with DNA (Figure 2.2) (Garcia et al., 1970; Pai et al., 1981; Inami et al., 2009).

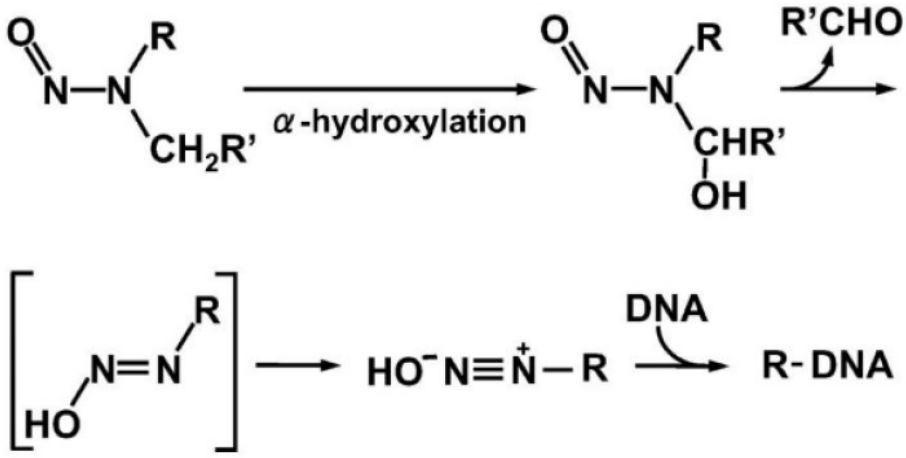

Figure 2.2: Nitrosamine reactivity with DNA (Inami et al., 2009)

Nitrosamines in amine scrubbing were suggested as a potential problem by Rochelle et al. (2001) and reported in monoethanolamine systems (MEA) in 2003 (Strazisar et al., 2003). Stable nitrosamines form only in secondary amines, but it is possible for all amines to form nitrosamines by oxidative and thermal degradation. With a lot of research shifting towards piperazine (PZ) as an advanced solvent for amine scrubbing (Freeman et al., 2010), interest in nitrosamine mitigation from PZ systems has grown. PZ can form mononitrosopiperazine (MNPZ) and dinitrosopiperazine (DNPZ).

Although, a number of methods are available for nitrosamine control such as high temperature decomposition and reclaiming (Fine, 2015), many amines are thermally

unstable, limiting the stripper temperature below 120 °C. At low stripper temperature, the decomposition rate is lower, allowing nitrosamines to accumulate to potentially dangerous levels. Reclaiming might also not be viable if the amine is non-volatile, which is applicable to tertiary amines and amino acids. Other methods include hydrogenation or UV photolysis, but these processes require additional equipment and might not be economically viable.

A way around these difficulties would be to remove the nitrosating agents (NO, NO_2) upstream of the absorber before they react with the amine. Methods that have been used to remove these nitrosating agents are described in the upcoming sections.

2.2 METHODS OF NO_X AND SO_2 REMOVAL

To meet the emission requirements for SO_2 and NO_x , power plants may implement one of the following options: switching to a higher grade of coal, purchase allowances, or retrofit with conventional technology like limestone slurry scrubbing or lime spray drying (Nelli, 1997). Limestone slurry scrubbing accounts for more than 90% of the SO_2 removal equipment used at utility plants (Kuehn, 1993). It is widely used due to the level of commercial operating experience and potential for high SO_2 removal.

For NO_x removal, application of low-NO_x burner technology to existing boilers must be sufficient to meet compliance standards. Low-NO_x burner technology essentially creates a staged combustion effect within the boiler, giving rise to fuel-rich and fuel-lean zones that reduce the oxygen availability which in turn lowers NO_x emissions. Modifications of this sort typically reduce existing NO_x emissions by 40-70% (Wood, 1994). With NO_x regulations tightening as new low-NO_x technology is being developed, additional NO_x removal can only be achieved using a post-combustion process.

Currently, the two most common technologies used for post-combustion removal of NO_x are selective catalytic reduction (SCR) and selective non-catalytic reduction (SNCR). In SCR, ammonia is injected into flue gas to reduce NO_x to nitrogen and water. The reactions are catalyzed by a metal oxide catalyst at a temperature of 600-750 °F. Typically, SCR lowers NO_x emissions by 70-90% (Wood, 1994). SCR is an expensive process for existing plants, due to retrofitting costs and cost of replacing the catalyst bed. The installation cost of SCR typically ranges from $ 75 to $ 150/kW (Nelli, 1997). In the SNCR process, urea is injected into the furnace to reduce NO_x emissions. Although the chemistry of SNCR is similar to SCR, it requires temperatures in the range of 1600-2200 °F. It is not as effective as the SCR but is a much simpler process with a lower capital cost.

2.2.1 Dry Scrubbing

NO_x removal has been investigated using a number of potential duct injection systems using sodium bicarbonate (KVB, 1990), zinc oxide (Rosenburg and Nuzum, 1986), alkalized alumina (Medellin, 1978), and calcium silicate solids (Chu and Rochelle, 1989). However, these NO_2 removal experiments were conducted at conditions that were not indicative of typical flue gas conditions. For example, sodium bicarbonate was exposed to high concentrations of SO_2, NO_x (10% NO_2 and 90% NO) at a high temperature and no water content. This disadvantage propelled the research towards NO_2 and SO_2 removal using alkaline solutions.

2.2.2 Wet Scrubbing Using Alkaline Solutions

Among the wet technologies, NO_x removal by methanol injection followed by limestone slurry scrubbing is an attractive candidate. It offers several advantages over other technologies – it is economical, easy to retrofit to an existing plant to achieve simultaneous NO_x and SO_2 removal, and has low capital cost of equipment. Furthermore, limestone is

less expensive than lime. One other advantage of limestone slurry scrubbing is the possibility of simultaneous SO_2 and NO_2 removal. When SO_2 is absorbed into a calcium carbonate slurry, calcium sulfite is formed which reacts with the NO_2 to remove it from the gas phase. In the presence of oxygen and NO_2, calcium sulfite oxidizes to calcium sulfate, which can be land-filled along with small amounts of calcium nitrogen-sulfur compounds. Figure 2.3 shows a schematic of a limestone slurry scrubber with a retrofit strategy to oxidize NO to NO_2.

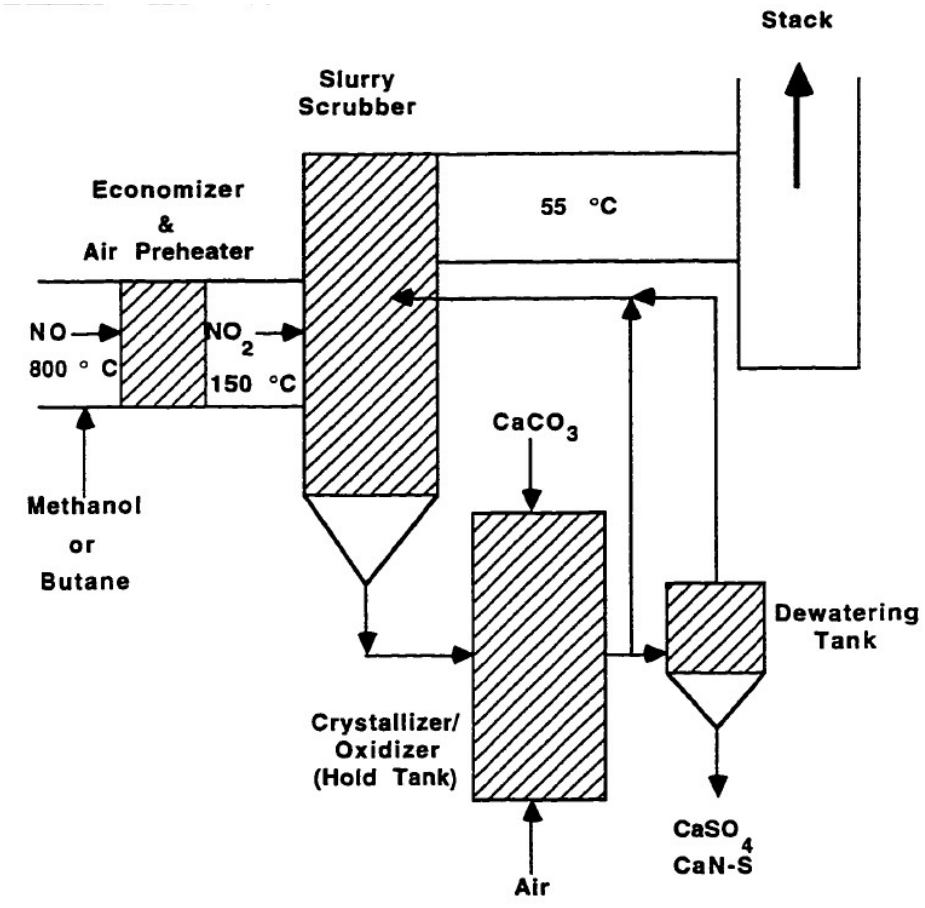

Figure 2.3: NO_x removal by limestone slurry scrubbing

Another method of wet scrubbing is reaction with NaOH. Hydrolysis of SO_2 in alkaline solutions (NaOH) produces the necessary concentration of S(IV) to react with

NO_2. Nash (1979) determined that such a reaction involved electron transfer leading to a chain mechanism of free radical. NO_2 has been proposed to react with sulfite in the following manner (Littlejohn et al., 1993):

$$NO_2 + SO_3^{2-} \rightarrow NO_2^- + SO_3^{-\bullet} \quad (2.1)$$

$$SO_3^{-\bullet} + SO_3^{-\bullet} \rightarrow SO_3^{2-} + SO_3 \quad (2.2)$$

$$SO_3 + H_2O \rightarrow SO_4^{2-} + 2H^+ \quad (2.3)$$

When the above reactions are combined, the following stoichiometry is obtained:

$$2NO_2 + SO_3^{2-} + H_2O \rightarrow 2NO_2^- + SO_4^{2-} + 2H^+ \quad (2.4)$$

NO_2 also reacts with bisulfite in a similar manner:

$$2NO_2 + HSO_3^- + H_2O \rightarrow 2NO_2^- + SO_4^{2-} + 3H^+ \quad (2.5)$$

Other species were also found in the liquid phase such as dithionate and a number of sulfur-nitrogen compounds such as hydroxylamine disulfonate, amine disulfonate, hydroxylamine, and sulfamic acid. Littlejohn et al. (1993) found small amounts of dithionate produced by the NO_2-sulfite reaction. The reaction responsible for dithionate production is shown below:

$$SO_3^{-\bullet} + SO_3^{-\bullet} \rightarrow S_2O_6 \quad (2.6)$$

An important side reaction between nitrite and bisulfite produces hydroxylamine disulfonate (HADS), which is an important precursor for a number of S-N compounds (Chang et al., 1982; Jarvis et al., 1985). HADS was the dominant S-N compound in the pH range 3-8. Jarvis et al. (1985) identified HADS and ADS (amine disulfonate) to be major S-N compounds in limestone slurry scrubbing. ADS was the most concentrated S-N compound under low pH conditions. These reactions are shown in Figure 2.4.

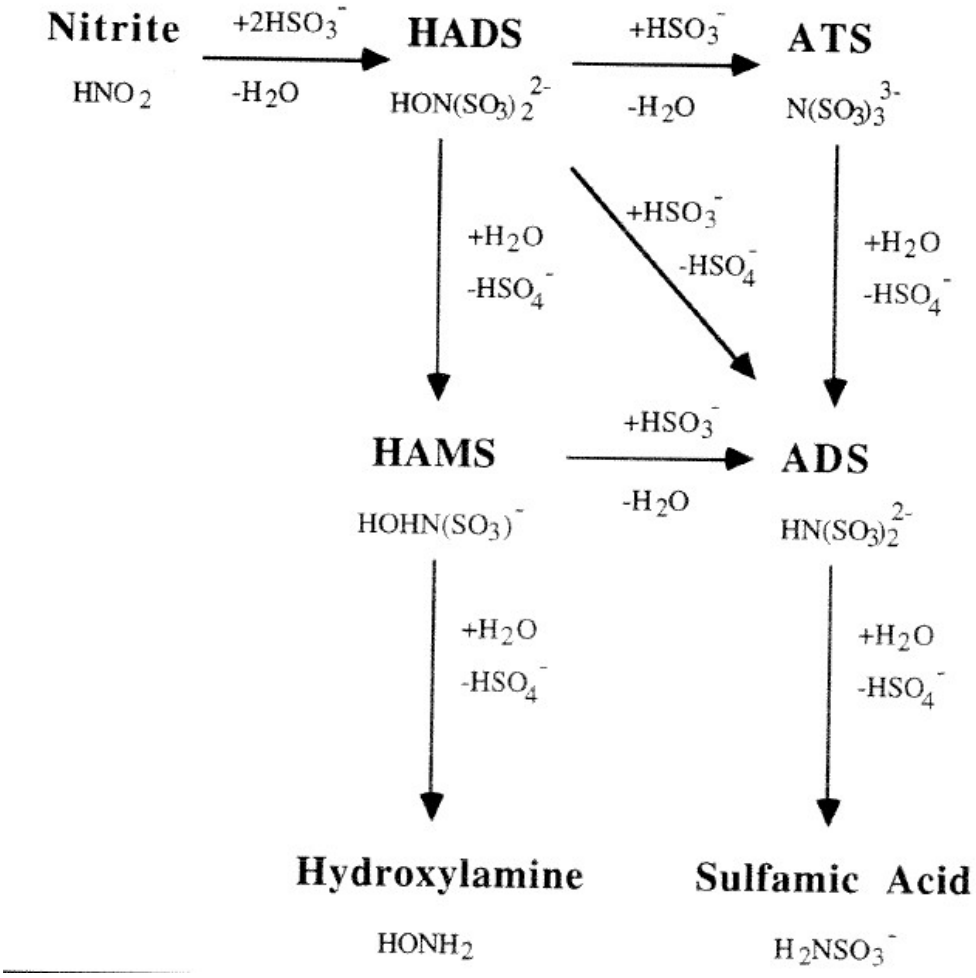

Figure 2.4: Sulfur-nitrogen reaction scheme (Chang et al., 1981)

2.3 SULFITE OXIDATION

Sulfite, in the presence of oxygen, is oxidized to sulfate. The oxidation of sulfite to sulfate is catalyzed by the presence of NO_2 (Littlejohn et al., 1993; Shen and Rochelle, 1995). Although a major fraction of the NO_x in the flue gas is NO, it does not readily dissolve in sulfite solutions and hence does not contribute to the oxidation of sulfite. NO_2 on the other hand is readily soluble in sulfite (Fine, 2015). Free radicals produced by the reaction of NO_2 with sulfite and bisulfite are involved in the oxidation of sulfite to sulfate (Equations 2.7 – 2.11).

$$NO_2 + SO_3^{2-} \rightarrow NO_2^- + SO_3^{-\bullet} \quad (2.7)$$

$$SO_3^{-\bullet} + O_2 \rightarrow SO_5^{-\bullet} \quad (2.8)$$

$$SO_5^{-\bullet} + SO_3^{2-} \rightarrow SO_4^{2-} + SO_4^{-\bullet} \quad (2.9)$$

$$SO_4^{-\bullet} + SO_3^{2-} \rightarrow SO_4^{2-} + SO_3^{-\bullet} \quad (2.10)$$

$$SO_3^{-\bullet} + SO_3^{-\bullet} \rightarrow S_2O_6^{2-} \quad (2.11)$$

From the above equations, for every mole of NO_2 absorbed, several moles of sulfite are oxidized to sulfate if oxygen is present. Oxygen is hence detrimental to the NO_2-sulfite reaction by reducing the amount of sulfite in the liquid phase. This in turn reduces the amount of absorbed NO_2, thereby reducing the removal. Takeuchi et al. (1977) observed that NO_2 removal decreased by 40% when air, instead of nitrogen, was used as the diluent for the feed gas. An explanation or mechanism to account for this observation was not provided but they tested the effect of additives such as EDTA-2Na, glycine, acetic acid and MEA on oxidation of sulfite. Shen (1997) showed that the presence of ferric ions (Fe^{2+}) even in trace amounts, provided another pathway for the oxidation of sulfite in solution.

To minimize the oxidation of sulfite, the effect of several antioxidants on the rate of sulfite-oxidation have been studied including hydroquinone (HQ), phenol, ethanolamines (MEA and DEA), ethylene glycol monoethyl ether, glycine, EDTA, and acetic acid. Sodium thiosulfate ($Na_2S_2O_3$) is another effective oxidation inhibitor because it is a free radical scavenger. It provides an alternative route for the termination of free radical mechanism of sulfite oxidation by competing with SO_3^{2-} in reacting with $SO_5^{-\cdot}$. The following mechanism was highlighted for the oxidation of sulfite in the presence of NO_2 and thiosulfate by Owens (1984).

$$NO_2 + SO_3^{2-} \rightarrow NO_2^- + SO_3^{-\bullet} \quad (2.12)$$

$$SO_3^{-\bullet} + O_2 \rightarrow SO_5^{-\bullet} \quad (2.13)$$

$$SO_5^{-\bullet} + S_2O_3^{2-} \rightarrow SO_5^{2-} + S_2O_3^{-\bullet} \quad (2.14)$$

$$SO_5^{2-} + SO_3^{2-} \rightarrow 2SO_4^{2-} \quad (2.15)$$

$$S_2O_3^{-\bullet} + S_2O_3^{-\bullet} \rightarrow S_4O_6^{2-} \quad (2.16)$$

Equation 2.12 was first outlined by Nash (1979) and Equations 2.13-2.16 were proposed by Huie and Neta (1984). Shen (1997) concluded that because NO_2 absorption is first order in sulfite, NO_2 removal is strongly affected by sulfite oxidation. The inhibition of sulfite oxidation can be done in both limestone slurry scrubbers and SO_2 polishing scrubbers using NaOH as the alkali. Major differences between the two are that the polishing scrubber runs at a higher pH and lower inlet SO_2 concentration than typical limestone slurry scrubbers. Limestone slurry scrubbers also contain high dissolved metals due to metal impurities in the limestone feed compared to NaOH feed in the polishing scrubber.

Fine (2015) investigated NO_2 catalyzed sulfite oxidation at conditions relevant to a typical NaOH polishing scrubber with: 7-135 mM sulfite, 0-100 mM thiosulfate, 2-10 ppm NO_2, Fe^{2+}/EDTA, 2-20% O_2 at 20-60 ℃. He concluded that sulfite oxidation is first order in sulfite, when normalized for the amount of NO_2 absorbed and half-order in NO_2 absorption for both inhibited and uninhibited systems. It was also verified that 25 mM thiosulfate reduced sulfite oxidation by a factor of 30 (Fine, 2015).

Selinger (2018) continued the experimentation of NO_2 absorption in sulfite at pilot-scale conditions in the National Carbon Capture Center in Wilsonville, Alabama. He successfully demonstrated 90% removal of NO_2 in a 1400-gallon pilot-scale prescrubber and concluded that pH is an important variable that affected NO_2 removal. Given 9000 lb/hr of flue gas with 5 ppm NO_2 and 40 ppm SO_2, a sulfite concentration of 25 mM is required to give an NO_2 removal of 90%. Under steady-state conditions, 50 mM thiosulfate was required to maintain 25 mM sulfite. Increasing the pH of the prescrubber solution by 1.5 units could increase removal by up to 8% (Selinger, 2018).

2.4 ECONOMICS OF THE SO_2 POLISHING SCRUBBER

Other agents of prescrubbing have been investigated by Fine (2015) and an economic analysis of the prescrubber was conducted by him. He concluded that under high inlet SO_2 conditions, NO_2 scrubbing using TEA (triethanolamine) becomes prohibitive due to the high purge rate from the prescrubber. NO_2 removal by sulfite, however, is cheaper under high SO_2 conditions as the SO_2 promotes the formation of sulfite. The savings realized from NO_2 prescrubbing are defined by the balance between the unrealized PZ losses and cost of thiosulfate required for oxidation inhibition. Amine degradation and cost of reclaiming can cost between $ 0.15-45/MT CO_2/ppm NO_2 (Fine, 2015). The cost of $Na_2S_2O_3$ feed is $ 0.03/ mol, but thiosulfate could be used at an even cheaper price if made

on site with emulsified sulfur (Lee and Benson, 1990). The following reaction was proposed by them for the *in situ* production of thiosulfate in the prescrubber:

$$S + SO_3^{2-} \rightarrow S_2O_3^{2-} \tag{2.17}$$

According to Donaldson and Johnson (1969), the above reaction was first order in sulfur and independent of pH or sulfite concentration when the pH was above 5.0. Other methods to produce thiosulfate *in situ* are by dissolving sulfur in sulfide solutions (Gould, 1962). However, this method was found to cause serious odor problems by the liberation of H_2S due to the formation of a local low pH spot in the solution despite the alkaline bulk solution. This reaction is shown in Equation 2.18.

$$S_X^{2-} + HSO_3^- \rightarrow S_{X-1}^{2-} + S_2O_3^{2-} + H^+ \tag{2.18}$$

Hence, polysulfide usage was abandoned in the EPA limestone scrubbing pilot plant at Research Triangle Park (RTP) (Lee and Benson, 1990). Safer methods of producing thiosulfate are adding polysulfides to prescrubbers along with lime slurries. The high pH of the feed and scrubbing solution as well as the fast dissolution of lime will prevent the formation of H_2S by neutralizing the proton in Equation 2.18.

2.5 SCOPE OF THIS WORK

This work extends previous work done on NO_2 absorption using SO_2 polishing scrubbers by using sulfur to produce thiosulfate *in situ* for the inhibition of sulfite oxidation. Particularly, this work aims to test the applicability of sulfur in the prescrubber at the National Carbon Capture Center, Alabama by running rigorous bench-scale

experiments at the University of Texas at Austin. There has been no prior experience or data related to applying emulsified sulfur at the prescrubber conditions pertaining to NCCC.

In these bench-scale experiments, 3 types of sulfur – emulsified, granular, and powdered have been compared on the basis of their thiosulfate yield, reactivity, and ease of applicability and the best form of sulfur has been chosen. Other experiments have been conducted to test the effect of ionic strength, pH, and temperature on the rate of reaction between sulfur and sulfite. Also, factorial bench-scale experiments have been conducted to come up with a rate law equation for the reaction. Finally, an existing bench-scale test apparatus has been modified to test the applicability of sulfur at volumetrically scaled down NCCC prescrubber gas flow rates. At the pilot-scale, thiosulfate has been tested in two campaigns at NCCC – Coal, 2018 and NGCC, 2019, with varying gas flow rate, NO_2 concentration, and SO_2 concentration to test the effect of buffer tank liquid hold-up and pH on NO_2 removal and sulfite oxidation.

Chapter 3: Methods

This chapter provides a description of the analytical methods and experimental methods used in this chapter. The analytical methods are focused on liquid phase analysis of anions and the experimental methods cover the bench and pilot-scale set-up used to carry out experiments. Most apparatuses and experimental methods were created by previous researchers and were only slightly modified in the context of this work. Newly developed or modified methods have been explained in sufficient detail to reproduce the research.

3.1 ANALYTICAL METHODS

3.1.1 Anion Chromatography

The analysis for anions was done using a Dionex ICS-3000 anion chromatograph with an IonPac AS15 (Sexton 2008; Freeman 2011). The chromatograph separates anions based on their strength in an adsorption column as the eluent gradually displaces them from adsorption sites. The eluent contained 2 to 45 mM potassium hydroxide (KOH) in analytical grade DDI water generated by an eluent generator at 1.6 mL/min. The separation of anions occurred in an IonPac AG15 guard column (4 x 50 mm) and IonPac AS15 analytical column (4 x 250 mm) (Nielsen, 2018). The resulting peaks were integrated and compared with calibration curves to estimate the original concentration of anions in the sample. This method was used to quantify the amount of sulfite, sulfate, thiosulfate, nitrate, and nitrite in both bench-scale and pilot plant samples. All samples were diluted 100-1000x gravimetrically in water prior to analysis. The samples were also fixed with formaldehyde (2 g of 35 wt% HCHO / 10 g of pilot sample; 100 µL of 35 wt% HCHO / 1 mL of bench scale sample) to convert the oxidatively unstable sulfite to methylsulfonic acid (MSA) (Equation 3.1). The elution times for sulfite, sulfate, and thiosulfate were 14, 15, and 22

minutes, respectively (Figure 3.1). The instrument was calibrated over the range of 0-100 mM for sulfite and thiosulfate and in the range of 0-1000 mM for sulfate.

$$HCHO + SO_3^{2-} + H_2O \rightarrow HCHOHSO_3^- + OH^- \quad (3.1)$$

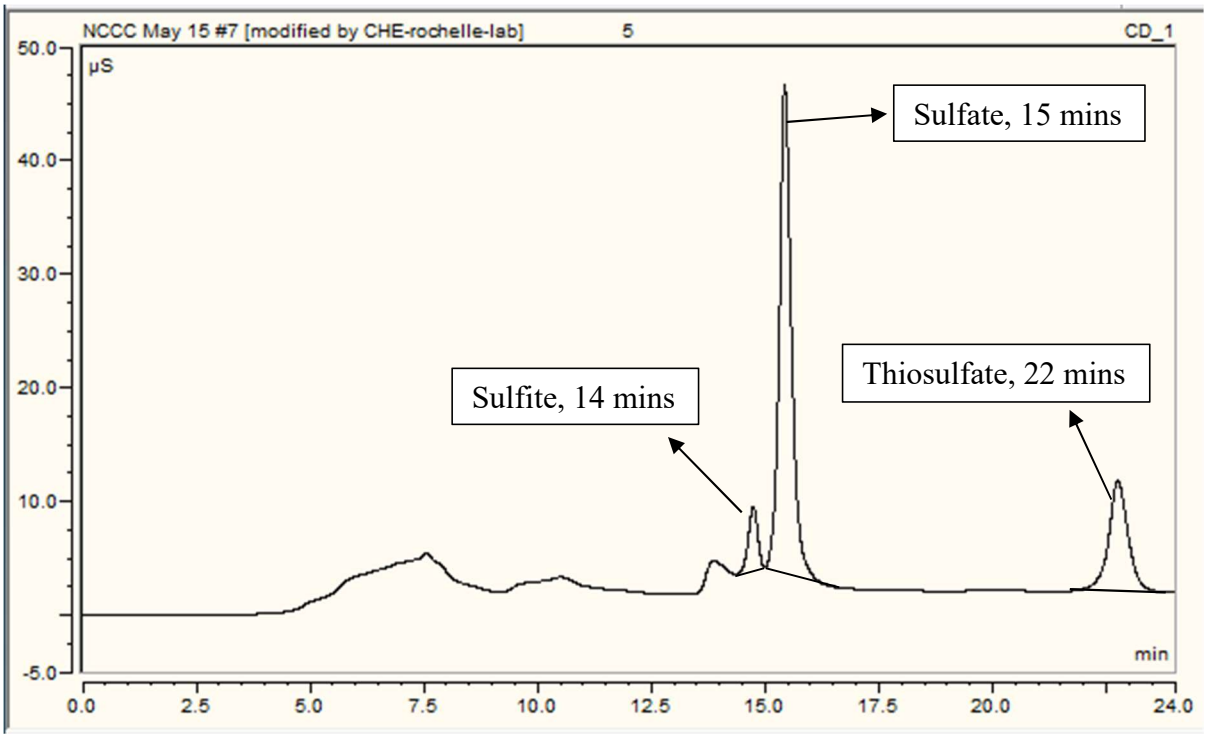

Figure 3.1: Anion chromatography peaks for sulfite, sulfate and thiosulfate (100 x dilution, sample fixed with 2 g of 35 wt% formaldehyde per 10 g of sample)

3.1.2 Inductively-Coupled Plasma Spectroscopy (ICP-OES)

ICP-OES was used to quantify the liquid-phase concentration of elements in the samples. In pilot plant samples, ICP-OES was used to quantify the amount of Na, Li, K, Cr, Fe, Mn, Ni, Se, and Hg. The ICP-OES equipment measured the metal concentrations by quantifying the emittance of a sample when exposed to UV light of a specified wavelength in an argon plasma flame at 7000 K. A Varian 710-ES Axial ICP-OES (Varian

Inc., Palo Alto, CA) was used in this analysis. Prior to analysis, samples were diluted by a factor of 25x gravimetrically in 2 vol% aqueous nitric acid in 15 mL centrifuge vials (Nielsen, 2018). The total sodium was useful in preparing the bench-scale reactor solution for long-term simulation experiments of the pilot plant prescrubber. Lithium concentration was important to track the water mass balance in the low gas flow reactor.

For each element, two to three wavelengths that gave the highest intensity were measured along with one argon wavelength as background. Calibration samples were prepared for each individual element between 0.5 and 25 ppm_w from a Fischer Scientific 1000 µg/mL AA standards diluted in 2 vol% HNO_3 for each run.

Table 3.1: Characteristic wavelengths for ICP-OES metals quantification (Nielsen, 2018)

Element Analyzed	*Measure Wavelengths (nm)*		
Argon (Ar)	737.212		
Iron (Fe)	234.350	238.204	259.940
Chromium (Cr)	205.560	206.158	267.716
Nickel (Ni)	216.555	221.648	231.604
Manganese (Mn)	257.610	259.372	260.568
Copper (Cu)	213.598	224.700	324.754

3.1.3 Total Alkalinity Analysis

The total alkalinity analysis was used to confirm the concentration of pilot plant solvent used in the prescrubber and was performed using a Metrohm Titrando series automatic titrator. Computer software was used to operate the titrator and record data. Samples were volumetrically diluted 300x by mixing 60 mL DDI water with 0.2 g of sample in a glass beaker. The potentiometric probe was submerged in the sample and

automatic doses of 0.1 mL of 0.2 N aqueous sulfuric acid were added to the sample in 10 second intervals to bring the pH down to 2.4. The equivalence points and required acid dosage were automatically detected and recorded by the software. Total alkalinity was then calculated by dividing the product of the volume of acid required to reach equivalence and the acid normality, by the mass of sample.

3.1.4 Emulsified Sulfur Analysis

Turbidity was used to calculate the total sulfur concentration in the bench-scale samples. Turbidity is a measure of the cloudiness of the solution. This cloudiness is caused by the fine emulsified sulfur particles dispersed in solution. The cloudiness is related to the size of sulfur particles, which reduces as the reaction between sulfur and sulfite proceeds. Turbidity was important both to estimate the conversion of sulfur to thiosulfate and to track the mass balance on sulfur in the low gas flow reactor. Measurements were made using an Oakton T-100 turbidimeter. Turbidity was measured in Nephelometric Turbidity Units (NTU). The effect of temperature on turbidity was neglected in this research.

A linear relation between sulfur concentration and turbidity was observed (Figure 3.2). This linear relation held true irrespective of ionic strength. For all experiments, pure DDI water was assumed to have a turbidity of zero. Hence, if the initial solution turbidity is known, a linear correlation between NTU and sulfur could be obtained for a given experiment. This correlation was then used to track the change in sulfur concentration throughout the experiment.

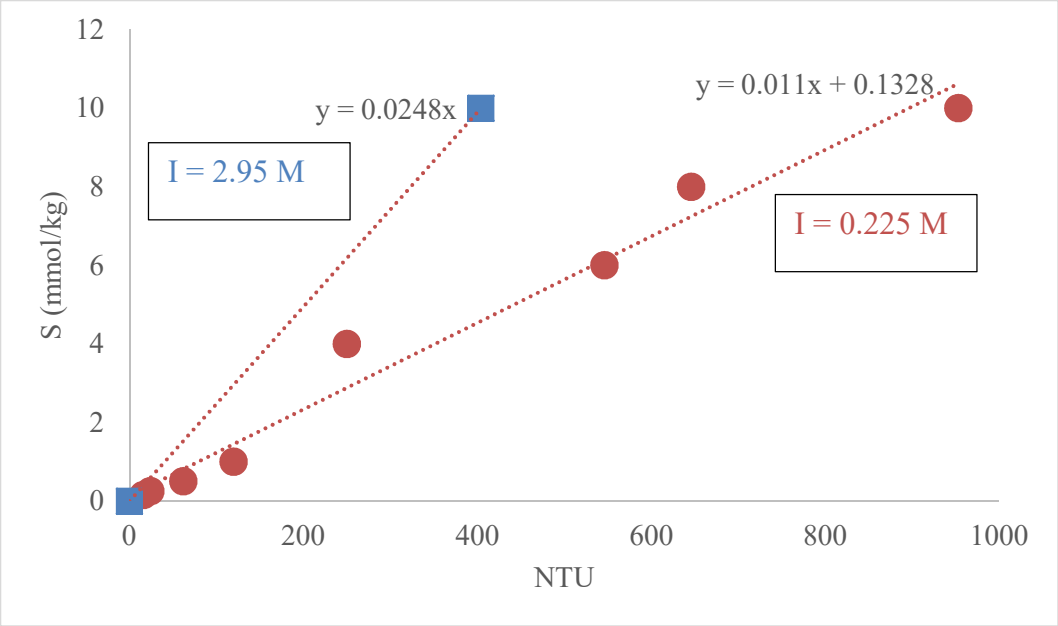

Figure 3.2: Sulfur concentration linearly correlated with turbidity at different ionic strengths (55 °C, 0.1M CO_3^{2-}/0.1M HCO_3^-, 25 mM SO_3^{2-}, 50 mM $S_2O_3^{2-}$, rest SO_4^{2-})

Prior to analysis, two calibrations had to be done – one for the instrument itself and one using a sample taken at time zero of the experiment. The former calibration was done using stock solutions of turbidities 800, 200, 20, and 0.08 NTU respectively. The latter calibration was important because a sample with a given concentration of sulfur would have different turbidities depending on the ionic strength of the solution.

3.2 EXPERIMENTAL METHODS

3.2.1 Low Gas Flow Reactor Setup

The low gas flow reactor setup was used to carry out bench-scale experiments. The schematic is shown in Figure 3.3. The setup consists of a 1 L jacketed glass reactor that is heated using an oil circulated heater. The reactor contained a 0.5 L solution of varying concentrations of sulfur, sulfite, thiosulfate, and sulfate depending on the type of

experiment conducted. This solution was vortexed at 500 rpm in the presence of the gas using a motorized stirrer. The initial pH of the solution was adjusted by using an equimolar mixture of 0.1 M CO_3^{2-}/0.1 M HCO_3^- as buffer.

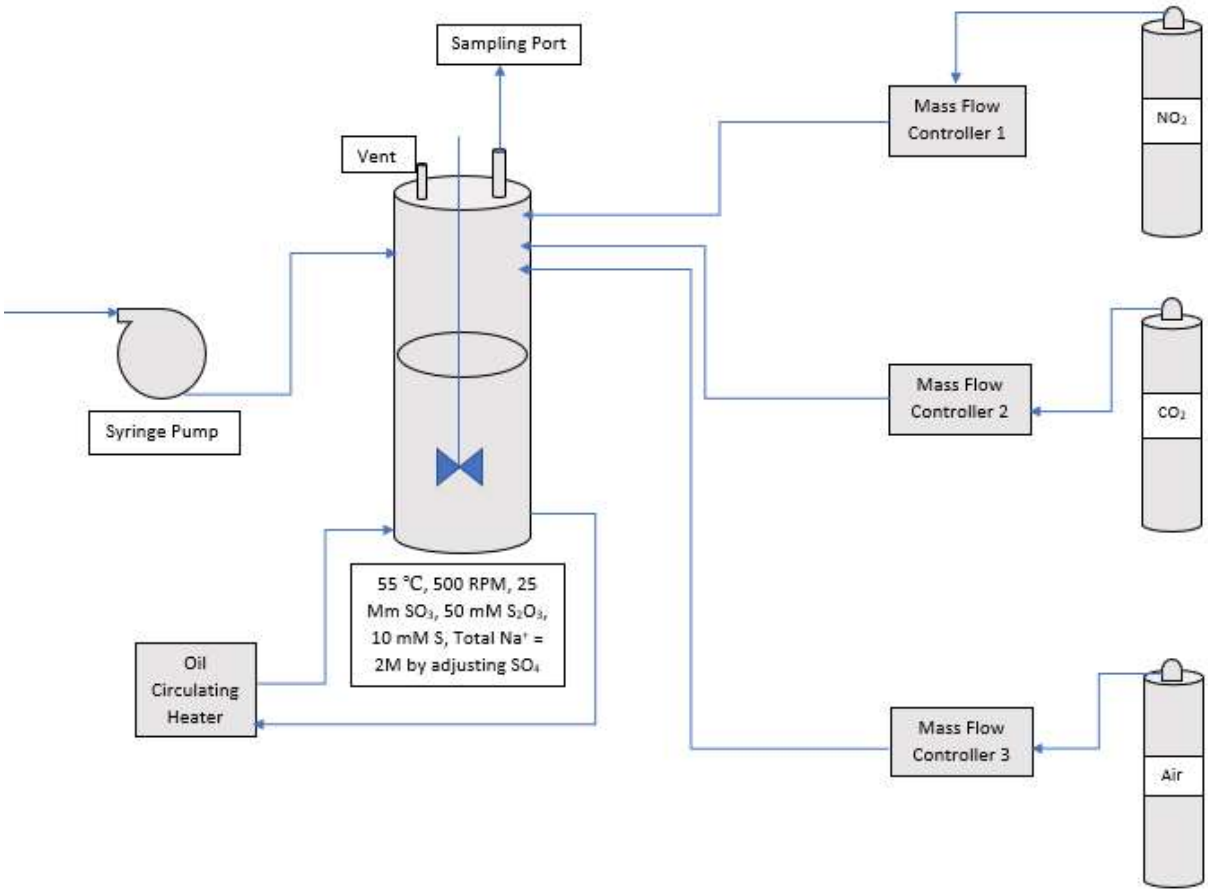

Figure 3.3: Modified low gas flow reactor set up

The temperature of the reactor was maintained at 55 ℃ for all experiments to closely match the temperature of the pilot plant prescrubber. The reactor accepted gas lines for CO_2, air, NO_2, and N_2 as required by the experiment type. Before entering the reactor, the gas stream containing CO_2, air, and N_2 entered a saturator to saturate the gas with water at 55 ℃ (15% H_2O). This stream was the mixed with the NO_2 stream separately and sent

into the top of the reactor. The flowrates of the gases were regulated using carefully calibrated mass flow controllers.

pH and temperature of the reactor were monitored throughout the duration of experiments and the reactor was sampled every hour after an initial sample was taken closely after the reaction began. The specific aspects of the different experiments tested on this equipment are given below.

3.2.1.1 Initial Screening Experiments

Screening experiments were conducted at the very beginning of this research to select a type of sulfur that is most suitable for this research to be commercially applied. Characteristics of the sulfur that factored into this decision were its phase, conversion to thiosulfate, reactivity with sulfite, and ease of processing in a commercial setup. The sulfur sources compared were powdered sulfur, emulsified sulfur, and granular sulfur. The emulsified sulfur was purchased from Martin Midstream Partners, Kilgore, Texas. Granular sulfur was purchased from Seed World USA, Odessa, Florida. Powdered sulfur was purchased from Alpha Chemicals.

All screening experiments were conducted using 0.5 L solution of 10 mM S, 25 mM SO_3^{2-} and 50 mM $S_2O_3^{2-}$ buffered with 0.1 M CO_3^{2-}/0.1 M HCO_3^- at 55 °C with a total Na^+ concentration of 2 M to simulate pilot plant conditions. These conditions will be referred to as "base" conditions for simplicity. The total sodium concentration of 2 M was achieved by adding sodium sulfate. There was no gas flow in these experiments. The reactivity of the solid sulfur types was measured by calculating the difference in sulfur mass before and after the experiment. Emulsified sulfur reactivity was calculated using turbidity measurements.

3.2.1.2 Effect of Ionic Strength

The pilot plant prescrubber solution has a greater ionic strength (2.95 M) compared to the bench-scale solution (0.225 M). The reaction of sulfur with sulfite is affected by the environment in which the sulfur is present. To test this effect, the ionic strength of the bench-scale solution was varied over the range of 0.225-3.7 by varying the sulfite concentration while keeping the thiosulfate at 50 mM, sulfur at 10 mM, and buffer at 0.1 M CO_3^{2-}/0.1 M HCO_3^- at 55 ℃. Again, the total sodium concentration was maintained at 2 M by adjusting the concentration of sulfate in each of these experiments. A total gas flowrate of 100 mL/min of 12% CO_2 in N_2 was used.

3.2.1.3 Effect of Temperature

To estimate the effect of temperature and derive an Arrhenius activation energy for the reaction between sulfur and sulfite, the kinetics was evaluated at three different temperatures – 40 ℃, 55 ℃, and 75 ℃. All the other aspects of the process were held at 10 mM S, 25 mM SO_3^{2-}, and 50 mM $S_2O_3^{2-}$ buffered with 0.1 M CO_3^{2-}/0.1 M HCO_3^- at 55 ℃ with a total Na^+ concentration of 2 M. The gas flow was maintained at a total of 100 mL/min of 12% CO_2 in N_2.

3.2.1.4 Factorial Experiments and Rate Law

The objective of conducting factorial bench-scale experiments was to derive a rate law equation for the reaction of sulfur with sulfite in the presence of thiosulfate. Eight two-level factorial experiments were designed in which the independent variables were the sulfite, sulfate, and thiosulfate. The experimental design is shown below in Table 3.2.

Table 3.2: Two level three factorial design of experiments (55 °C, 0.5 L, 500 rpm, Na^+ = 2M)

Experiment #	S (mM)	SO_3^{2-} (mM)	$S_2O_3^{2-}$ (mM)	SO_4^{2-} (mM)
1	10	25	50	775
2	10	25	100	725
3	10	50	50	750
4	10	50	100	700
5	20	25	50	775
6	20	25	100	725
7	20	50	50	750
8	20	50	100	700

The interpreted rate of the reaction was calculated as the rate of loss of sulfur (in mM) with time. In all the experiments, a total sodium concentration of 2 M was maintained by adjusting the sulfate concentration. The experiments were conducted at 55 °C with the buffer being 0.1 M CO_3^{2-}/0.1 M HCO_3^- and a total gas flow of 100 mL/min of 12% CO_2 in N_2.

3.2.1.5 Long-Term Bench-Scale Simulation Experiments

The low gas flow reactor setup was modified by including a syringe pump to feed 7 wt% sulfurous acid in place of SO_2 gas. This was done to simulate the reaction between SO_2 and alkali using the reaction between H_2SO_3 and HCO_3^-/CO_3^{2-}. To simulate the pilot-scale-prescrubber, the actual pilot plant gas flowrate was scaled down volumetrically (Equation 3.2). The individual gas flowrates reflected the typical concentrations of the gases entering the prescrubber under coal flue gas (12% CO_2) conditions.

$$\left(\frac{Q}{V}\right)_{Pilot} = \left(\frac{Q}{V}\right)_{Benc} \tag{3.2}$$

The remaining aspects of these experiments remained constant at "base" conditions. In these experiments, the sulfur and the anions were tracked with time unlike previous experiments where the interest was only on the rate of reaction rate. This was necessary in order to predict bench-scale sulfite and thiosulfate degradation rates prior to pilot plant campaigns and compare them with pilot plant degradation. The advantage of running bench-scale simulations of pilot-scale conditions is having the ability to tweak process conditions and predict pilot plant performance or to gain knowledge about how to better operate the pilot plant prescrubber.

3.2.2 Pilot Plant Prescrubber

Pilot-scale experimentation was done at the National Carbon Capture Center in Wilsonville, Alabama. The experiments were carried out in a SO_2 polishing scrubber with 1400-gallon solution inventory under both coal (12% CO_2) and NGCC (4% CO_2) conditions. The coal-fired flue gas contained 12% CO_2, 7% O_2, 0 ppm SO_2 and 0-5 ppm NO_2. Solvent (10 wt% NaOH) was constantly circulated between the prescrubber column and a buffer tank at 1500 lb/hr. Figure 3.4 shows a simplified process flow diagram showing the prescrubber, buffer tank, chemical addition, and disposal. The prescrubber is 30 inches in diameter with one section of Mellapak Plus 252Y structured packing. The packing height is 20 feet.

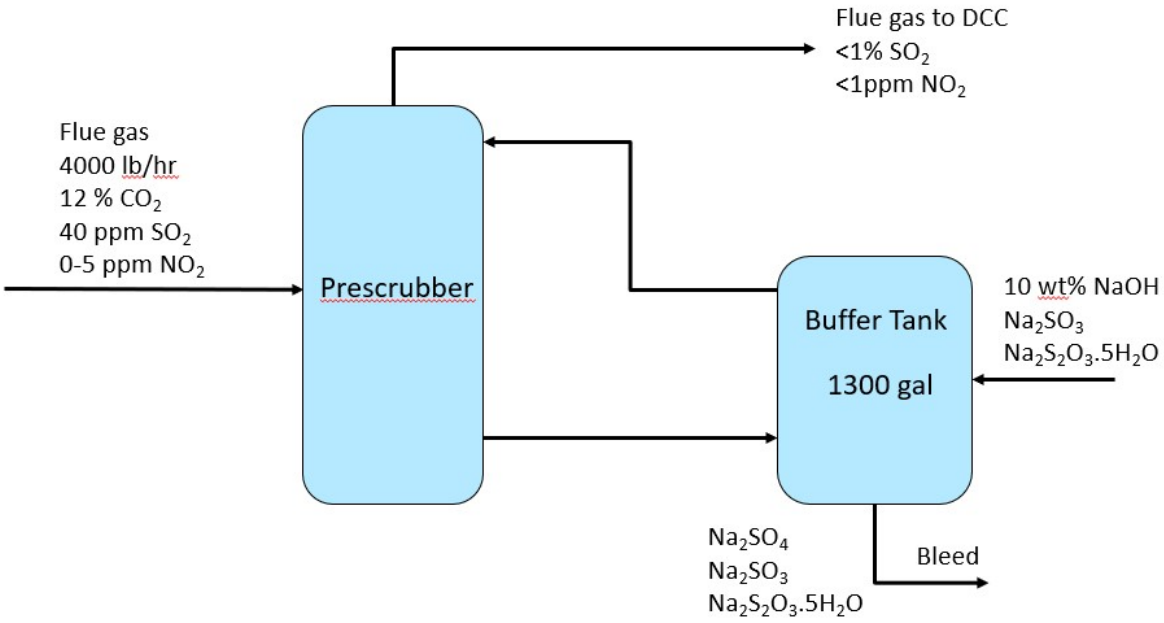

Figure 3.4: Pilot plant prescrubber and buffer tank set up

Previous experiments in the prescrubber were conducted at a gas flowrate of 9000 lb/hr with 1-5 ppm NO_2 under coal fired conditions. These experiments concluded that with 5 ppm NO_2 in the feed gas, 50 mM of thiosulfate is required to maintain 25 mM sulfite in the buffer tank to ensure the desired removal of NO_2 (90%) (Selinger, 2018). This specification was used as a basis for experiments conducted in this research work. In this work, experiments were conducted at coal fired conditions with a lower gas flowrate (4000 lb/hr) at low NO_2 conditions (0-1 ppm), and NGCC conditions (5000-8000 lb/hr gas) with 0-1 ppm NO_2 and low SO_2 (< 25 ppm).

The coal condition experiments at low gas flowrate were conducted with the objective being the reduction of sulfite oxidation in the scrubber by maintaining a high pH (> 8) (Selinger, 2018) and low solvent inventory in the column. To achieve these conditions, the tank level was drained at the beginning of the campaign to 20% and

increased to 45% by adding 110 lb of sodium thiosulfate pentahydrate along with 10 wt% NaOH.

At these conditions, the thiosulfate concentration was 85 mM which is well above the required 50 mM to ensure 25 mM sulfite in the tank for 90% NO_2 removal (Selinger, 2018). Thereafter, the system was left undisturbed and the pH, tank level, and NO_2 removal were monitored continuously. When pH dropped below 8.0, tank level was again drained to 20% and the addition of NaOH and thiosulfate were repeated like before, resulting in a net tank level of 45%. The buffer tank was sampled every week and samples were fixed with formaldehyde on site to prevent the oxidation of sulfite and analyzed at UT Austin for anions using Ion Chromatography.

NGCC condition experiments were conducted in Spring 2019 using the remaining undisturbed solvent inventory from Summer 2018. This resulted in almost complete oxidation of sulfite to sulfate resulting in less than 5 mM SO_3 at the beginning. Thiosulfate, however, was greater than 40 mM indicating that there might be other process conditions besides the thiosulfate concentration that need to be altered to maintain the sulfite concentration. Due to the sulfite and SO_2 coming into the prescrubber, NO_2 removal was much lower than 90% for most of the campaign. On May 3, 52 lb of sodium sulfite and 110 lb of sodium thiosulfate pentahydrate were added in order to make up for the low SO_2 in the feed gas. The prescrubber was sampled every two days throughout the campaign and samples were fixed with 2 g of 35 wt% formaldehyde per 10 g of sample on site to arrest the oxidation of sulfite. Samples were then shipped to UT Austin to analyze for sulfite, sulfate, and thiosulfate using anion chromatography.

NO_x analysis in both the campaigns was done using a Rosemount™ CT5100 Continuous Gas Analyzer that used a mid-infrared optical absorption spectroscopy technique to measure gas concentration. The detection range was 0-100 ppmv for NO_2 and

0-200 ppmv for NO. The results were reproducible with ± 1% error. The device was installed at the inlet of the prescrubber in the coal campaign and at the outlet of the prescrubber for the NGCC campaign.

Chapter 4: Results and Discussion

4.1 BENCH-SCALE RESULTS

4.1.1 Screening Experiments

Table 4.1 shows the thiosulfate yield after 50 hours of reaction from three sources of sulfur – powdered, emulsified, and granular. Emulsified sulfur, a liquid phase sulfur, gave the maximum conversion (in terms of concentration) to thiosulfate of 50%. Figure 4.1 shows the conversion of emulsified sulfur as a function of t/t_{50}. t_{50} is the time taken for the sulfur concentration to reach half its initial value. Emulsified sulfur was the most reactive form of sulfur with t_{50} being 6 hours. Emulsified sulfur can therefore be used in commercial units owing to its high reactivity and ease of use. Moreover, compared to the residence time in the prescrubber buffer tank at NCCC, the t_{50} is much smaller, indicating that the reaction of sulfur with sulfite can proceed to completion.

Table 4.1: Comparison of thiosulfate yield from sulfur sources (55 °C, 10 mM S, 25 mM SO_3^{2-}, 50 mM $S_2O_3^{2-}$, 500 rpm)

Sulfur source	Thiosulfate yield ([S in thiosulfate] / [S originally present]) (%)	Reactivity
Powdered	30	Partially unreactive
Emulsified	50	Completely reactive (t_{50} = 6 hrs)
Granular	16	Almost unreactive

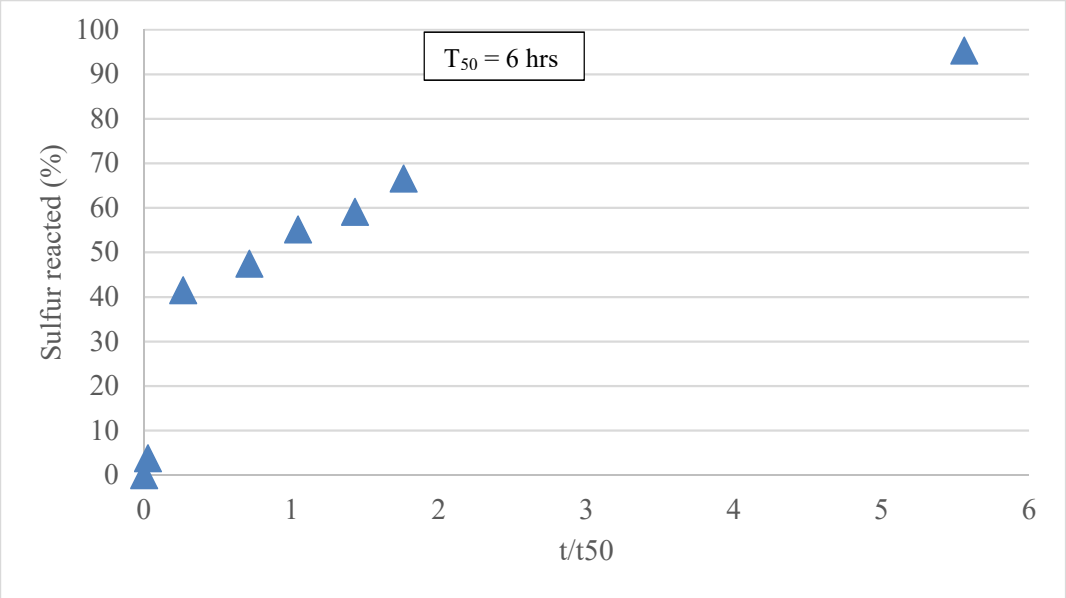

Figure 4.1: Emulsified sulfur conversion as a function of time normalized by the half-life

4.1.2 Effect of Ionic Strength

The rate of reaction between sulfur and sulfite decreased with increasing ionic strength. This reaction rate was interpreted as the rate of loss of sulfur with time, assuming the reaction was first order in sulfur. The prescrubber buffer tank solution had a high ionic strength of 2.95 M while the bench-scale tests were conducted at a low ionic strength of 0.225 M. The reaction rate at 0.225 M was 3 times as fast as the rate at 2.95 M (Figure 4.2). The residence time calculated in the buffer tank using a solvent inventory of 1300 gal and a flow rate corresponding to 10 mM S in 1500 lb/hr total solvent flow rate (usually), is in the order of weeks. Hence, while the reaction rate seems slow, the residence time in the prescrubber is much larger than in the bench-scale test apparatus. Hence, the reaction rate at high ionic strength should also be sufficiently fast to make it possible to use emulsified sulfur in commercial units.

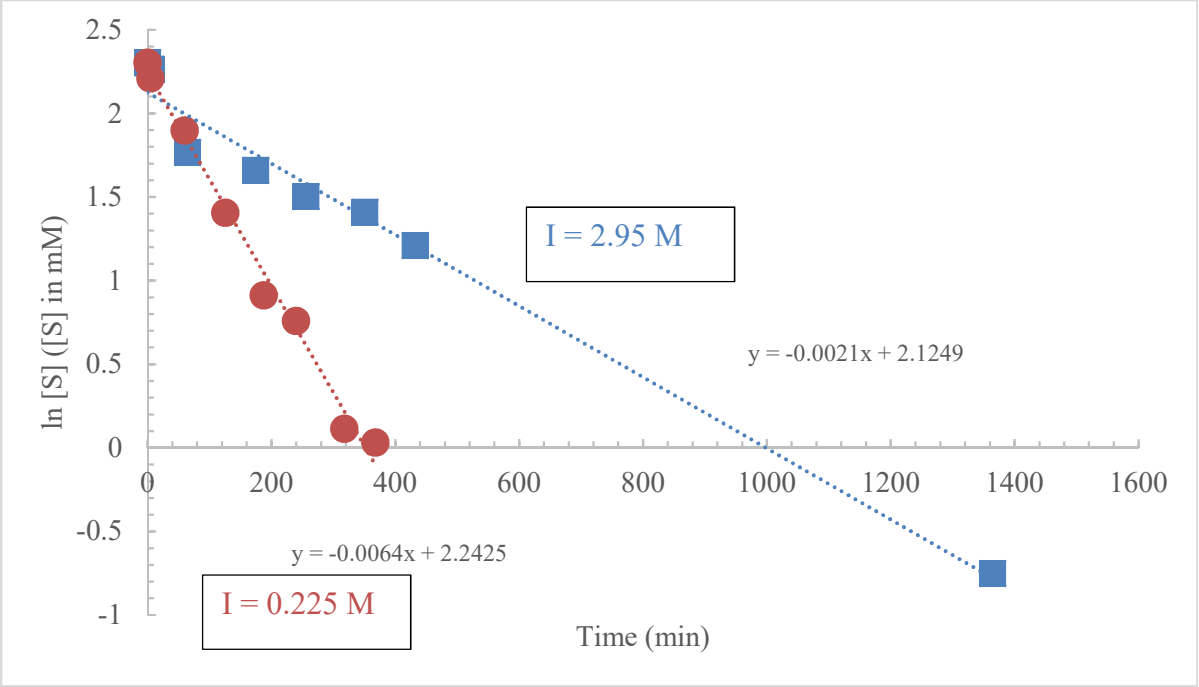

Figure 4.2: Rate of reaction of emulsified sulfur decreases with increase in ionic strength (55 °C, 25 mM SO_3^{2-}, 50 mM $S_2O_3^{2-}$, balance SO_4^{2-}, pH = 11.5)

4.1.3 Effect of temperature on reaction rate

Table 4.2 shows the effect of temperature on the rate of reaction. All reaction rate constants were interpreted as the rate of disappearance of sulfur. It is apparent from Table 4.2 that, at higher temperature, there is an increased reaction rate. The rate constant increased by a factor of 17 when the temperature was increased from 40 °C to 75 °C. This effect can be particularly useful in plants where the prescrubber is operated at higher than 55 °C. This result also means that the temperature of the prescrubber can be elevated to make up for the effect of high ionic strengths on the reaction rate.

Table 4.2: Effect of temperature on reaction rate (55 °C, 10 mM emulsified S, 25 mM SO_3^{2-}, 50 mM $S_2O_3^{2-}$, 2 M Na^+ adjusted using SO_4^{2-}, 0.1 M HCO_3^- / 0.1 M CO_3^2).

Temperature (°C)	Interpreted reaction rate constant (min^{-1})
40	$1.0x10^{-3}$
55	$2.0x10^{-3}$
75	$17\ x10^{-3}$

The temperature dependence of the rate constant was assumed to follow the Arrhenius equation and an Arrhenius activation energy was obtained from Figure 4.3. The value was found to be 74.2 kJ/mol, which is a high value, indicating that the reaction of emulsified sulfur with sulfite could be kinetically limited and not mass transfer dependent.

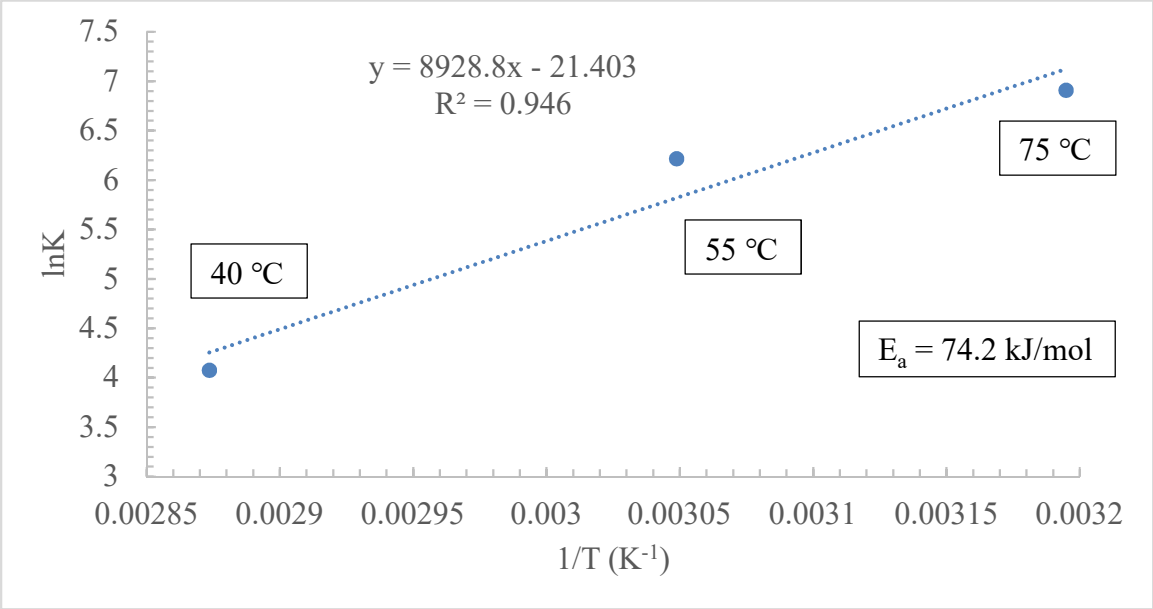

Figure 4.3: Arrhenius dependence of reaction rate on temperature (55 °C, 10 mM S, 25 mM SO_3^{2-}, 50 mM $S_2O_3^{2-}$, 2 M Na^+ adjusted using SO_4^{2-}, 0.1 M CO_3^{2-}/0.1 M HCO_3^-)

4.1.4 Rate Law Equation

To ascertain the dependence of the reaction rate on the concentrations of sulfur, sulfite and thiosulfate, factorial experiments were conducted, and the results of these experiments are shown in Table 4.3. Due to the assumption that the rate is first order in sulfur, the independent variable was chosen to be the rate of the reaction normalized by the sulfur concentration (or the first order rate constant) and the two independent variables were sulfite and thiosulfate.

Table 4.3: Two level three factorial design of experiments (55 °C, 0.5 L, 500 rpm, Na^+ = 2M)

Experiment #	S (mM)	SO_3^{2-} (mM)	$S_2O_3^{2-}$ (mM)	SO_4^{2-} (mM)	r' (min^{-1})
1	10	25	50	775	0.0021
2	10	25	100	725	0.0018
3	10	50	50	750	0.0026
4	10	50	100	700	0.0029
5	20	25	50	775	0.0018
6	20	25	100	725	0.0018
7	20	50	50	750	0.0028
8	20	50	100	700	0.0023

Equation 4.1 shows the model of rate equation and its parameters.

$$r' = r/[S] = k[SO_3]^{\alpha}[S_2O_3]^{\beta} \quad (4.1)$$

where:

r' = normalized rate
r = actual reaction rate
[S] = sulfur concentration
k = rate constant
$[SO_3]$ = sulfite concentration
$[S_2O_3]$ = thiosulfate concentration
α = order with respect to sulfite
β = order with respect to thiosulfate

The data shown in Table 4.4 was regressed linearly on Microsoft Excel. It was found that the reaction is half order in sulfite ($\alpha = 0.5$) and zero order in thiosulfate ($\beta = 0$) with a k value of 5.48 x 10^{-3} $mM^{-0.5}$ min^{-1}. Thiosulfate order was found to have a very weak and statistically insignificant dependence on the rate and hence β was 0. The k value and the sulfite order were found to be statistically significant from the ANOVA results shown in Table 4.4.

Table 4.4: ANOVA table showing statistical significance of estimated parameters.

Parameter	*Coefficients*	*Standard Error*	*t Stat*	*P-value*	*Lower 95%*	*Upper 95%*
ln K	-7.509	0.520	-14.424	2.89E-05	-8.847	-6.171
SO_3 order	0.496	0.093	5.310	0.003	0.256	0.737
S_2O_3 order	-0.087	0.093	-0.931	0.394	-0.327	0.153

Thus, the rate law equation for the reaction of sulfur with sulfite can be written as follows.

$$r = 5.48 \times 10^{-3}[S][SO_3]^{0.5} \quad (4.2)$$

Figure 4.4 shows a scatter plot of the experimentally measured rates versus the rate law model predicted values. There is a good agreement between the experimental and model predicted values with the absolute average deviation being 6.5%.

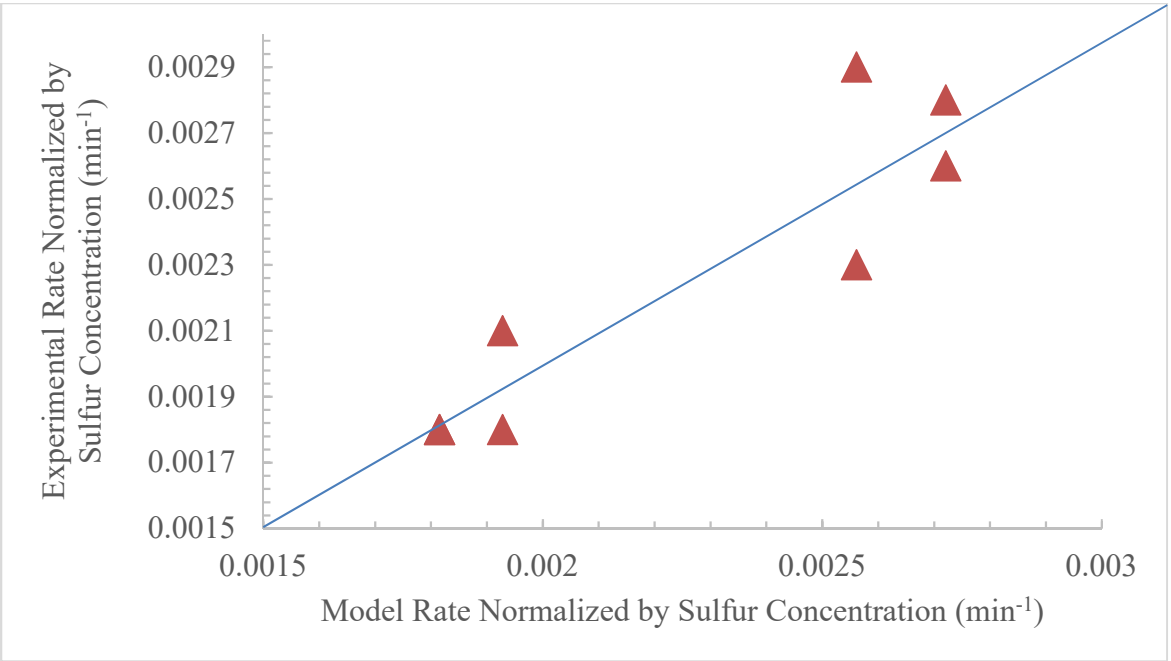

Figure 4.4: Experimental versus model-predicted normalized reaction rates for factorial experiments

4.2 PILOT-SCALE RESULTS

4.2.1 Coal Campaign

Figure 4.5 shows the pH and tank level as a function of time on the first day of pilot scale experimentation. Following the addition of 10 wt% NaOH and 110 lb of sodium thiosulfate pentahydrate at about 225 minutes, pH jumps to 12.2 and the tank level reaches 45%. With time, the tank level reaches a steady state around 44% but pH decreases immediately due to the reaction of CO_2 with NaOH. The tank level was not allowed to exceed 50% volume in this campaign in order to minimize thiosulfate degradation by minimizing solvent inventory. The average inventory through the test period was 456 gal.

Three main linear regions can be observed in the pH profile. In the first linear region (AB), pH drops the fastest from 12.2 to 9.8. A slight change in the slope of the line is

observed at around 300 minutes which could be due to the delayed effect of thiosulfate addition. In the second region (BC), pH drops at a much slower late, from 9.8 to 9 in 8 hours. This region corresponds to the conversion of carbonate ions to bicarbonate ions. In the final region CD, the pH gradually decreases from about 9 to 8.8, ultimately reaching 8 after a period of 2.5 weeks. One possible explanation for the different reaction times observed in the three linear pH regions could be the differences in the rates of the reactions depicted in Figure 4.5.

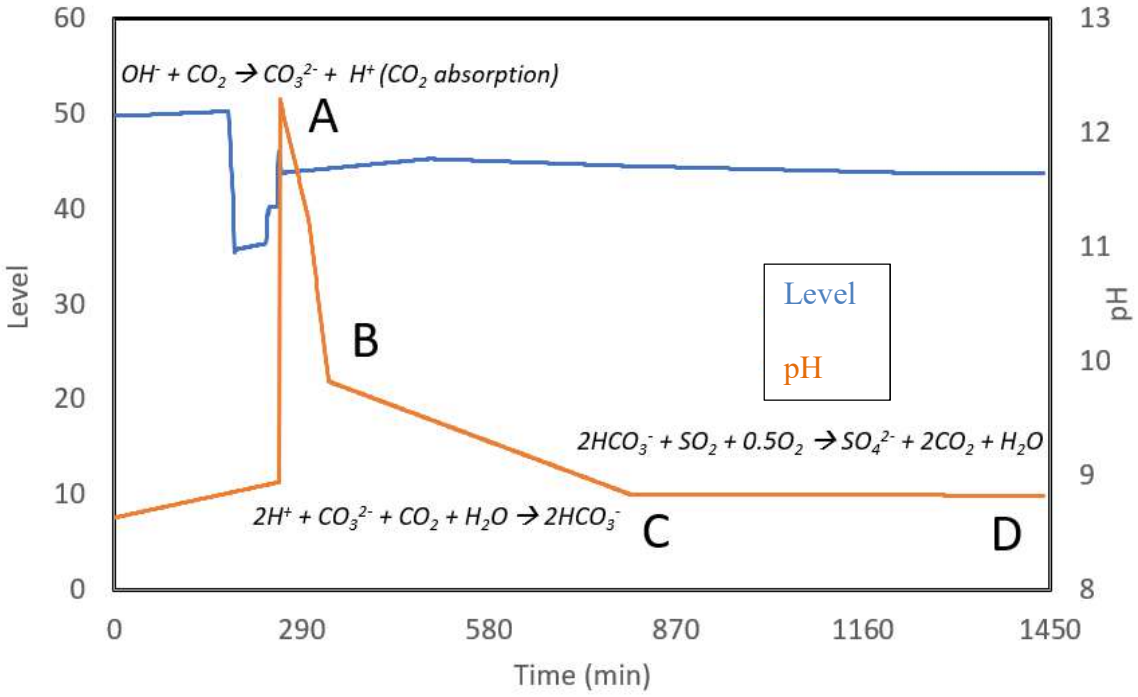

Figure 4.5: pH and level trends observed in NCCC prescrubber for coal campaign with characteristic reactions shown in linear regions

Figure 4.6 is a comparison of thiosulfate degradation rates under low and high NO_2 conditions. The two experiments depicted differ in the amount of flue gas processed as well as the NO_2 concentration. It was observed that under low NO_2 conditions (low flue gas), the oxidation rate of thiosulfate was 0.13 gmol/hr which was about half the interpreted

degradation rate under high NO_2, high gas flow rate conditions (Selinger, 2018). The flue gas processed for the high NO_2 experiments was about 2.25 times that of the low NO_2 experiments. This result also meant that more water vapor condensed in the prescrubber in the former case. As a consequence of this condensation, more thiosulfate was lost through tank bleed (60 gmol) under high gas conditions compared to 17.2 gmol for the low gas conditions.

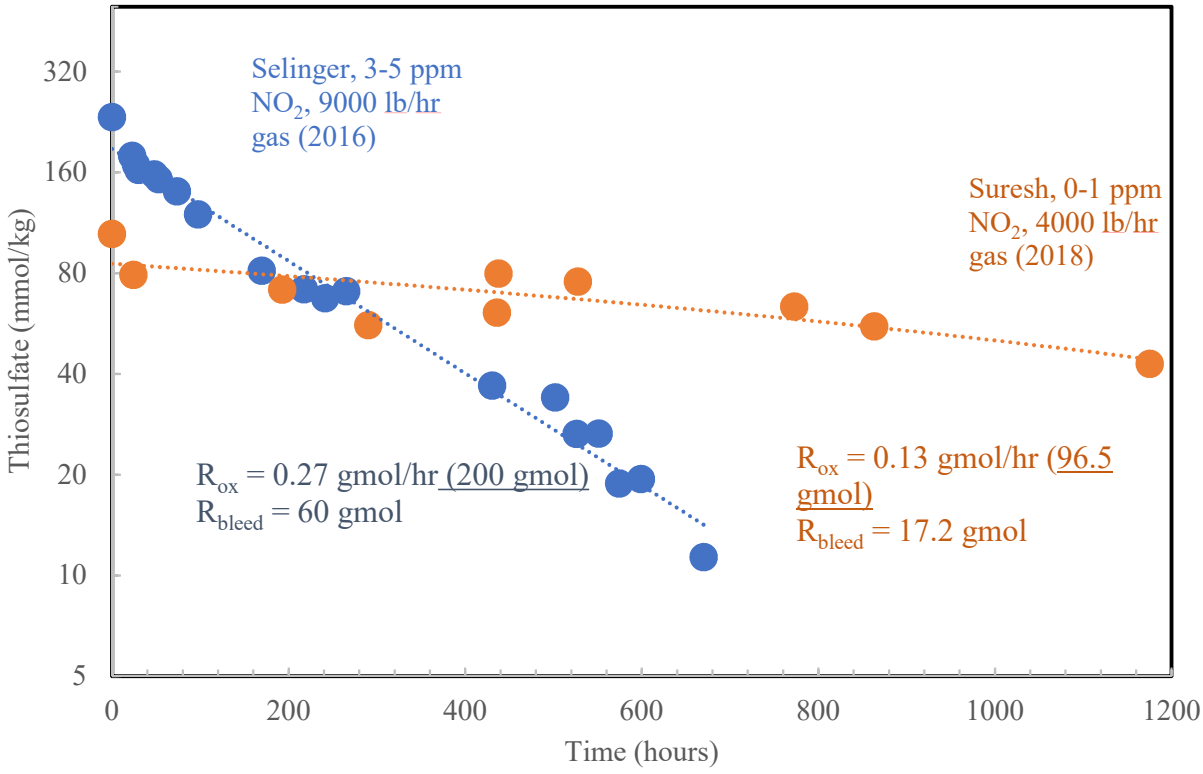

Figure 4.6: Thiosulfate degradation rates observed under 0-5 NO_2 conditions (orange) and 0-1 ppm NO_2 conditions (blue)

Figure 4.7 shows the relation between NO_2 removal and sulfite observed during the coal campaign in 2018. Previous pilot tests have shown that a minimum of 25 mM sulfite is required to maintain a NO_2 removal of 90% (Selinger, 2018). This sulfite concentration

can be maintained by consistently maintaining the thiosulfate concentration in the prescrubbber above 50 mM. From Figure 4.7, we can conclude that this minimum thiosulfate requirement is true even in the case of low NO_2 and low SO_2 conditions. For all points in the campaign where the sulfite was above 25 mM, there was a consistent removal of above 90%. When sulfite dropped below 25 mM, NO_2 removal also dropped to about 76%. There is however a consistent decrease in NO_2 removal that is observed irrespective of fluctuations in sulfite. This could be attributed to changes in pH which have also been proven to affect NO_2 removal (Selinger, 2018).

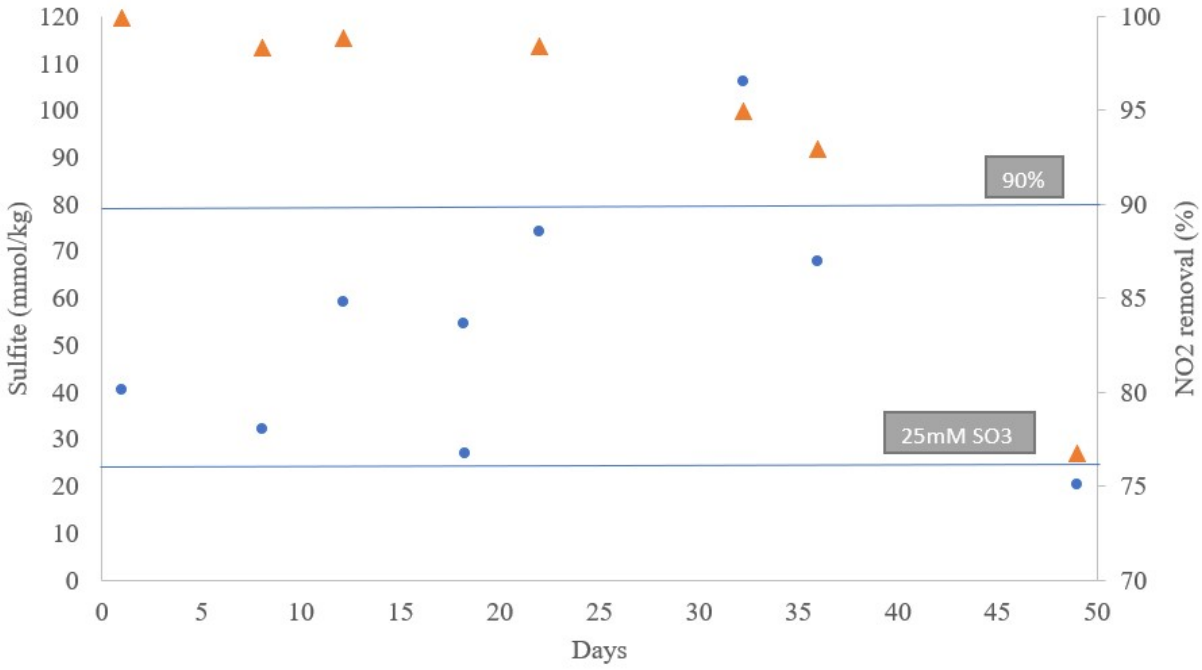

Figure 4.7: NO_2 removal and sulfite as a function of time in the coal campaign 2018 (0-1 ppm NO_2, 4000 lb/hr flue gas, 12% CO_2, 55 °C)

4.2.1 NGCC Campaign

The main differences in this campaign compared to earlier campaigns were the flue gas flow rate and the flue gas O_2 and SO_2 content. Flue gas flow rate was 3500 lb/hr which was greater than that of the coal campaign. Moreover, the flue gas that contained 12% CO_2 was diluted with air to give 12% CO_2, 7% O_2, and 8-33 ppm SO_2. NO_2 concentration remained around 0-1 ppm but NO_2 removal was not monitored carefully in this campaign due to unreliable gas measurements. The solvent inventory in this campaign was much higher than in the coal campaign, at an average of 826 gallons through the test period. There were also differences in the way the prescrubber was operated in this campaign. Unlike the coal campaign, solvent inventory was not reduced at the beginning of the campaign. pH and tank level were undisturbed throughout the campaign. pH remained between 8 and 9 throughout the campaign and tank level reached a maximum of 71% in this campaign. These results can be seen in Figure 4.8.

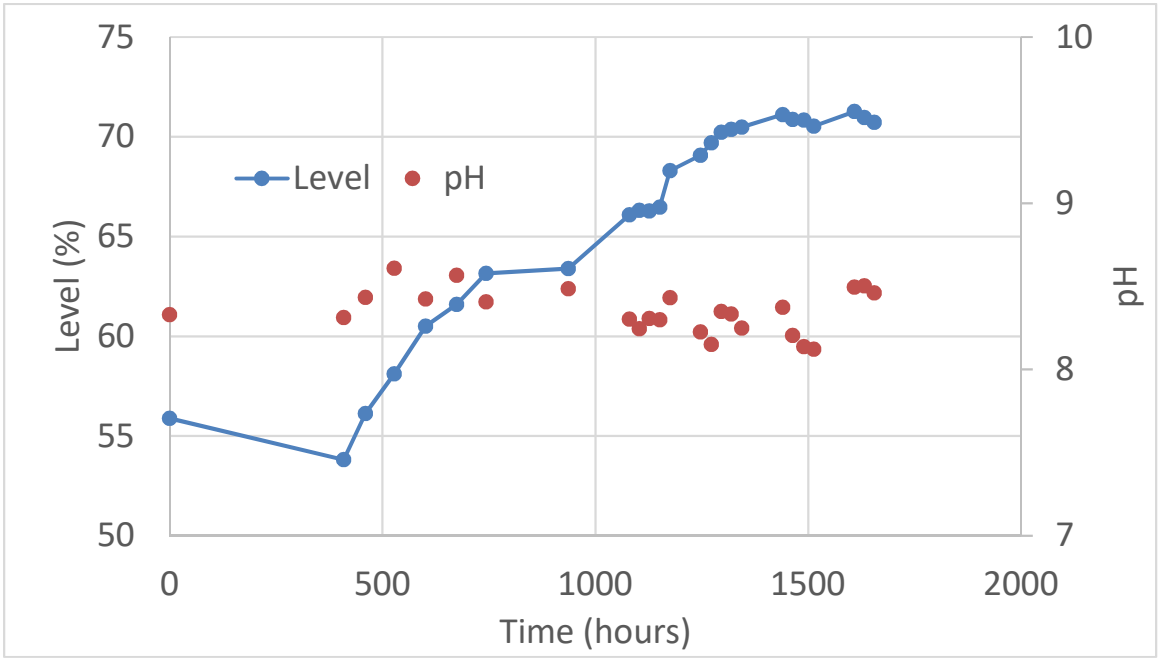

Figure 4.8: pH and level profile through the NGCC campaign

The solvent inventory was left undisturbed after the coal campaign which resulted in almost complete oxidation of sulfite. Hence, this campaign began with no sulfite and approximately 50 mM thiosulfate in the buffer tank. No other additional sulfite or thiosulfate was added at the beginning. Moreover, the incoming SO_2 concentration was much lower at 8 ppm resulting in very low conversion to sulfite. To compensate for this, 52 lb of sodium sulfite was introduced to the tank after about 980 hours of operation to give a sulfite concentration equivalent to 40 ppm SO_2. This followed by the addition of 55 lb of sodium thiosulfate to give a resulting thiosulfate concentration of 84 mM.

Figure 4.9 shows thiosulfate degradation rates before and after the addition of thiosulfate. Prior to thiosulfate addition at about 1000 hours, thiosulfate degraded at a rate of 0.112 gmol/hr. Following addition, the rate increased to 0.127 gmol/hr which was comparable to the thiosulfate degradation rate of 0.13 gmol/hr in the coal campaign, also with 0-1 ppm NO_2.

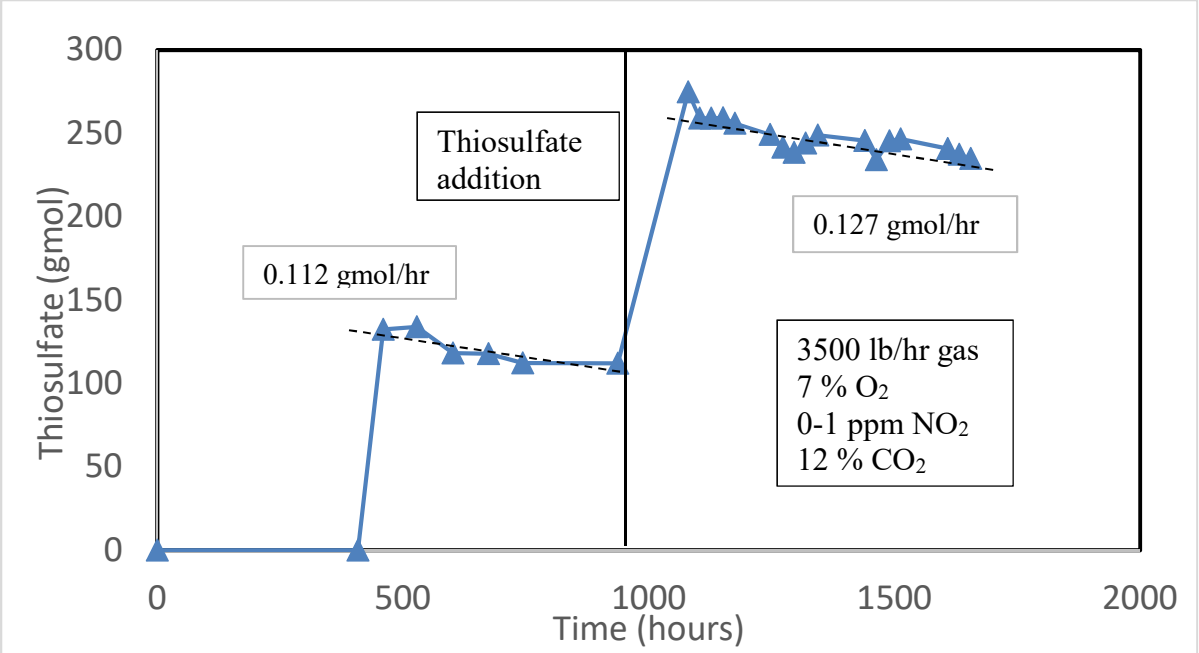

Figure 4.9: Thiosulfate degradation rates before and after thiosulfate addition (3500 lb/hr flue gas, 7% O_2, 0-1 ppm NO_2, 12% CO_2, 55 ℃)

Unlike previous campaigns, the NGCC campaign did not have 40 ppm SO_2 coming into the prescrubber. Figure 4.10 shows the SO_2 inlet to the prescrubber with time. The SO_2 coming into the prescrubber in the first 700 hours of operation was almost constant, with the average concentration being 10 ppm. After 700 hours, until the end of the campaign, SO_2 concentration increased to 33 ppm.

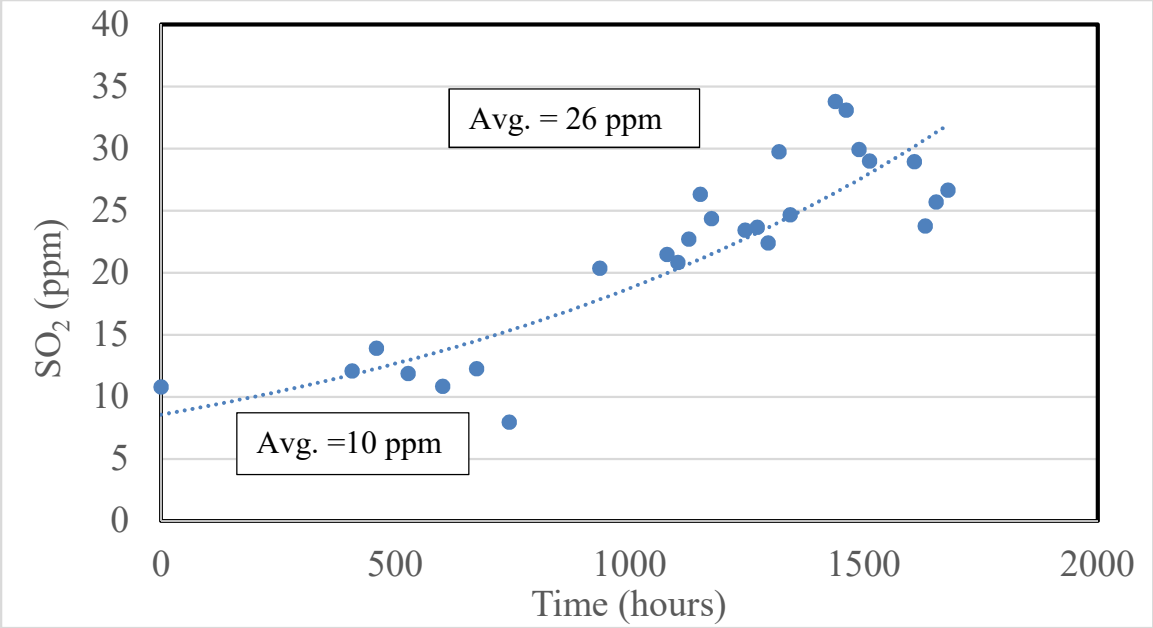

Figure 4.10: Prescrubber inlet SO_2 concentration as a function of time (3500 lb/hr flue gas, 7% O_2, 0-1 ppm NO_2, 12% CO_2, 55 °C)

Figure 4.11 shows the relation between thiosulfate and sulfite concentration in the prescrubber. The data correspond to the two different average SO_2 concentrations coming into the prescrubber. Until 700 hours, the SO_2 remained constant at 10 ppm and in this period, the sulfite and thiosulfate also remain constant. After 700 hours, an increase in the sulfite and consequently an increase in thiosulfate is seen. This is due to the increasing SO_2 coming into the prescrubber, with the average value at 26 ppm. A power law correlation is observed between thiosulfate and sulfite in this interval. However, this correlation cannot be used to obtain a minimum thiosulfate concentration from a given sulfite concentration to maintain 90% removal of NO_2 because NO_2 removal was not monitored in this campaign.

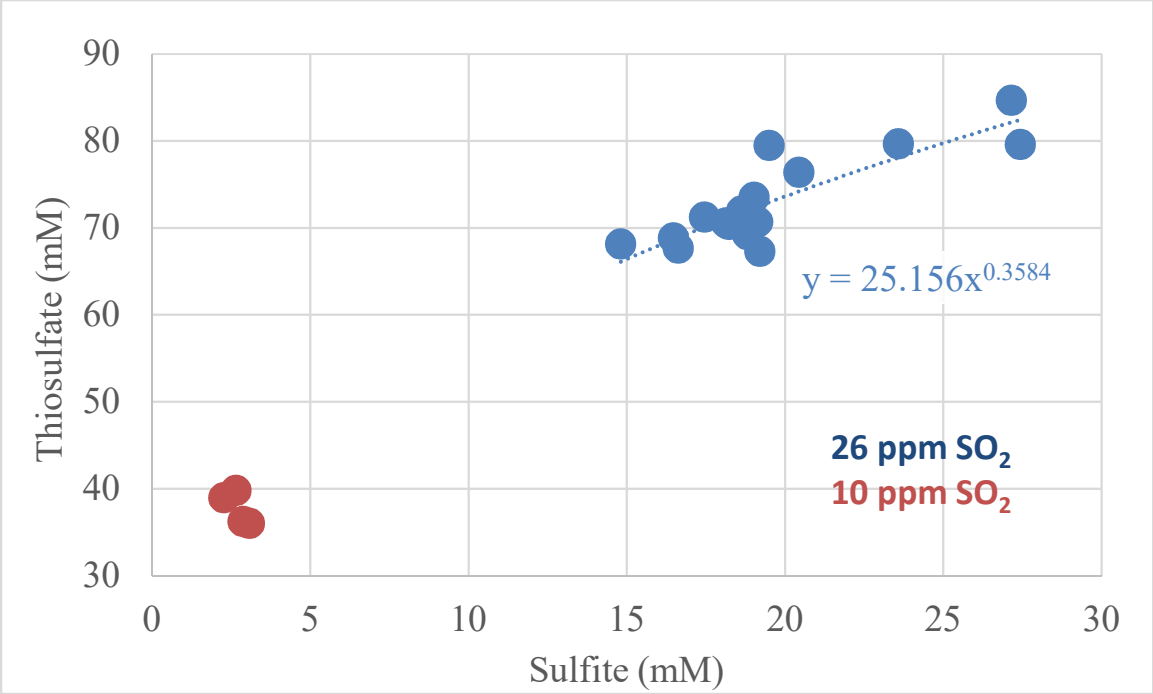

Figure 4.11: Relationship between thiosulfate and sulfite concentration at 10 ppm (red) and 26 ppm (blue) SO_2 (3500 lb/hr flue gas, 7% O_2, 0-1 ppm NO_2, 12% CO_2, 55 ℃)

The thiosulfate oxidation rates from both campaigns can be compared by treating NO_2 mole flow rate and solvent inventory as operating variables. When the rates and NO_2 mole flow rates are normalized by their respective average solvent inventories and compared, the following relation is obtained:

$$R_{ox} = 0.1717 * N_{NO2} + 0.00007$$

where:

R_{ox} = rate of thiosulfate oxidation normalized by solvent volume (lb/hr.gal)

N_{NO2} = NO_2 flow rate normalized by solvent volume (mol/hr.gal)

From the above equation, at very low NO_2 concentration, the thiosulfate oxidation rate can be extrapolated to be 0.00007 lb/hr.gal. This rate can be attributed to oxidation only by O_2 in the flue gas. The above model, however, takes into account only two data points from the two pilot plant tests conducted and hence can be modified or improved by conducting more pilot plant tests. Future testing can also include modeling the effect of oxygen in the flue gas.

Chapter 5: Conclusions and Recommendations

Chapter 5 outlines the conclusions that were drawn from the bench-scale and pilot-scale experiments that were explained in Chapters 3 and 4. Section 5.1 highlights conclusions from the bench-scale tests, Section 5.2 focuses on conclusions from pilot campaigns, and Section 5.3 gives recommendations for bench and pilot plant work on applying emulsified sulfur for *in situ* inhibition of sulfite oxidation in the prescrubber.

5.1 CONCLUSIONS FROM BENCH-SCALE EXPERIMENTS

- Emulsified sulfur was the most reactive form of sulfur with maximum conversion to thiosulfate of 50 % and a t_{50} of 6 hours, when compared to powdered and granular sulfur.
- Emulsified sulfur is a good candidate for pilot-scale application due to its small half-life compared to large typical prescrubber residence times and its ease of processing in large-scale plants.
- Turbidity of solution was linearly correlated with the sulfur concentration and can be used to quantify sulfur in bench and pilot plants to ensure the material balance closure on sulfur.
- Ionic strength has a profound effect on the rate of reaction between sulfur and sulfite. Reaction rate observed at typical prescrubber ionic strength was only 1/3 that of the bench-scale reaction rate.
- The dependence of reaction rate on temperature was found to follow the Arrenhius law with a high activation energy of 74.2 kJ/mol suggesting that the reaction could be kinetically limited and not mass-transfer dependent.

- The rate of reaction of sulfur with sulfite was found to be first order in sulfur, half order in sulfite, and zero order in thiosulfate, with a rate constant of 5.48 x 10^{-3} $mM^{-0.5}$ min^{-1}.
- Rate-law model-predicted rates matched experimentally determined values with an absolute average deviation of 6.5 %.

5.2 CONCLUSIONS FROM PILOT-SCALE EXPERIMENTS

- NO_2 concentration in the incoming flue gas directly impacted the rate of degradation of thiosulfate in the prescrubber. With 0-5 ppm NO_2 in the flue gas, the rate of thiosulfate degradation was 0.27 gmol/hr which was twice the degradation rate with 0-1 ppm NO_2, 0.13 gmol/hr.
- Volume-normalized thiosulfate oxidation rate was correlated with volume-normalized NO_2 mole flow rate. The thiosulfate oxidation rate in the absence of NO_2 was found to be 0.00007 lb/hr.gal.
- Larger gas flow rates could increase the required rate of replenishment of thiosulfate in the prescrubber due to the greater amount of water condensation. With 4000 lb/hr flue gas, the thiosulfate loss through tank bleed was 17.2 gmol compared to 60 gmol at 9000 lb/hr flue gas.
- 25 mM sulfite was observed to be the minimum sulfite concentration required to maintain NO_2 removal of 90 % even under low gas flow and low NO_2 conditions.
- The pH time profile in the prescrubber contained three linear regions corresponding to CO_2 absorption, bicarbonate formation, and CO_2 desorption. The characteristic times of these reactions resulted in different rates of pH change in these regions.

- Sulfite and thiosulfate concentration were directly correlated to the SO_2 concentration coming into the prescrubber.
- A power-law relation between thiosulfate and sulfite was observed even under low SO_2, low NO_2 conditions. The thiosulfate degradation rate by oxidation was found to be 0.127 gmol/hr with 0-1 ppm NO_2, 8-33 ppm SO_2, and 3500 lb/hr flue gas conditions.

5.3 RECOMMENDATIONS FOR FUTURE WORK

- Future work could involve including the effect of temperature on turbidity measurements while analyzing for emulsified sulfur. This research work assumed that turbidity was not a function of temperature.
- This research work assumed that sulfite, sulfate, and thiosulfate were the only sulfur products in the prescrubber. Future work could involve rigorously analyzing / developing analytical procedures for other compounds such as S-N compounds, trithionates, tetrathionates, and sulfides. Considering S-N compounds will ensure a better closure on the mass balance around sulfur.
- This research work ignores the formation of sodium sulfide when emulsified sulfur reacts with NaOH. Na_2S is very likely to form if sulfur is added to NaOH in the prescrubber at NCCC and hence is an important product in understanding sulfur reactions in the prescrubber.
- Potentially toxic emissions such as H_2S could occur when emulsified sulfur is used at the pilot scale and it is important to quantify the amount of these emissions beforehand. Future work can involve modifying the low gas flow

reactor for gas phase measurements for the measurement of H_2S from the reactor.

- Long term bench scale simulations of the pilot scale prescrubber must be conducted to quantify the effect of NO_2, sulfite, thiosulfate, pH, gas flow rate, CO_2 concentration, and SO_2 concentration on the applicability of emulsified sulfur for NO_2 scrubbing. This work had very little data from long-term bench-scale simulation experiments and focused mainly on setting up the simulation apparatus.
- Once bench-scale simulations have been conducted extensively, emulsified sulfur can be added to the pilot prescrubber to see its real time effect on NO_2 removal, thiosulfate production, and sulfite oxidation inhibition.
- A thorough economic analysis can be done to quantify the advantages of using emulsified sulfur in commercial prescrubbers instead of using sodium thiosulfate pentahydrate.
- Thiosulfate oxidation rate can be modeled by considering the effect of solvent inventory, NO_2 concentration, and O_2 concentration more rigorously.

References

Bland, V. V., and C. E. Martin. *Full-scale demonstration of additives for NO2 reduction with dry sodium desulfurization*. No. EPRI-GS-6852. Electric Power Research Inst., Palo Alto, CA (USA); KVB, Inc., Irvine, CA (USA), 1990.

Chang, Chung-Shih, and Gary T. Rochelle. "Effect of organic acid additives on SO2 absorption into CaO/CaCO3 slurries." *AIChE Journal* 28.2 (1982): 261-266.

Chang, Chung-Shih, and Gary T. Rochelle. "SO2 absorption into aqueous solutions." *AIChE Journal* 27.2 (1981): 292-298.

Chu, Paul, and Gary T. Rochelle. "Removal of SO2 and NOx from stack gas by reaction with calcium hydroxide solids." *Japca* 39.2 (1989): 175-179.

Donaldson, G. William, and Francis J. Johnston. "Reaction of colloidal sulfur with sulfite." *The Journal of Physical Chemistry*73.6 (1969): 2064-2068.

E. S. Gould, "*Inorganic Reactions and Structures*", *Revised Ed. pp. 291-292*, *1962.*

Fine, N. A. "Nitrosamine Management in Aqueous Amines for Post Combustion Carbon Capture. Ph. D. Dissertation." *The University of Texas at Austin* (2015).

Freeman, Stephanie A., et al. "Carbon dioxide capture with concentrated, aqueous piperazine." *International Journal of Greenhouse Gas Control* 4.2 (2010): 119-124.

Garcia, Humberto, et al. "Carcinogenicity of nitrosothiomorpholine and 1-nitrosopiperazine in rats." *Zeitschrift für Krebsforschung* 74.2 (1970): 179-184.

Huie, Robert E., and P. Neta. "Chemical behavior of sulfur trioxide (1-)(SO3-) and sulfur pentoxide (1-)(SO5-) radicals in aqueous solutions." *The Journal of Physical Chemistry* 88.23 (1984): 5665-5669.

Inami, Keiko, Satoko Ishikawa, and Masataka Mochizuki. "Activation mechanism of N-nitrosodialkylamines as environmental mutagens and its application to antitumor research." *Genes and Environment* 31.4 (2009): 97-104.

Jarvis, J. B., P. A. Nassos, and D. A. Stewart. "A Study of Sulfur-Nitrogen Compounds in Wet Lime/Limestone FGD Systems." *Proceedings, EPA/EPRI Symposium on Flue Gas Desulfurization*. 1985.

Kuehn, Steven E. "Utility plans take shape for Title IV compliance." *Power Engineering* 97.8 (1993): 19-27.

Lee, Yungli J., and Lewis B. Benson. "Sulfur dioxide removal from flue gases with sulfite oxidation inhibition." U.S. Patent No. 4,976,937. 11 Dec. 1990.

Littlejohn, David, Yizhong Wang, and Shih Ger Chang. "Oxidation of aqueous sulfite ion by nitrogen dioxide." *Environmental Science & Technology* 27.10 (1993): 2162-2167.

Medellin, Pedro M., Eric Weger, and Milorad P. Duduković. "Removal of SO2 and NOx from simulated flue gases by alkalized alumina in a radial flow fixed bed." *Industrial & Engineering Chemistry Process Design and Development* 17.4 (1978): 528-536.

Nash, T. "The effect of nitrogen dioxide and of some transition metals on the oxidation of dilute bisulphite solutions." *Atmospheric Environment (1967)* 13.8 (1979): 1149-1154.

Nelli, Christopher Herman. "Nitrogen dioxide removal by calcium silicate solids." (1998): 3785-3785.

Nielsen III, Paul Thomas. *Oxidation of piperazine in post-combustion carbon capture*. Diss. 2018.

Owens, David Richard. *Sulfite oxidation inhibited by thiosulfate*. Diss. University of Texas at Austin, 1984.

Pai, S. R., A. J. Shirke, and S. V. Gothoskar. "Long-term feeding study in C17 mice administered saccharin coated betel nut and 1, 4-dinitrosopiperazine in combination." *Carcinogenesis* 2.3 (1981): 175-177.

R. R. Bottoms (Girdler Corp.), "Separating acid gases," U.S. Patent 1783901, 1930.

Rosenberg, H. S., and H. K. Nuzum. *Development of a combined NOx/SO2 removal system based on ZnO scrubbing technology. Final report, 1 September 1983-30 September 1985*. No. DOE/PC/60264-T3. Battelle Columbus Labs., OH (USA), 1986.

Selinger, Joseph Leo. *Pilot plant modeling of Advanced Flash Stripper with piperazine*. Diss. 2018.

Sexton, Andrew James. *Amine oxidation in carbon dioxide capture processes*. Diss. The University of Texas at Austin, 2008.

Shen, C. H., and G. T. Rochelle. "NO2 Absorption in Limestone Slurry for Flue Gas Desulfurization." *Proceeding. The 1995 SO 2 Control Symposium*. 1995.

Shen, Chen Hua. *Nitrogen dioxide absorption in aqueous sodium sulfite*. 1997.

Strazisar, Brian R., Richard R. Anderson, and Curt M. White. "Degradation pathways for monoethanolamine in a CO2 capture facility." *Energy & fuels* 17.4 (2003): 1034-1039.

Takeuchi, Hiroshi, Makoto Ando, and Nobuo Kizawa. "Absorption of nitrogen oxides in aqueous sodium sulfite and bisulfite solutions." *Industrial & Engineering Chemistry Process Design and Development* 16.3 (1977): 303-308.

Wood, Stephen C. "Select the right NO_x control technology." *Chemical Engineering Progress* 90.1 (1994): 32-38.